Petrography and Geochemistry of Alkaline Rocks from Michni (Warsak), NW Pakistan

By

Muhammad Jawad Zeb

M. Phil

Department of Earth Sciences

Quaid-i-Azam University,

Islamabad

2023

ACKNOWLEDGEMENTS

All Glory to Almighty ALLAH Who has blessed me with the ability, capacity, and perseverance to finish this study.

I want to express my gratitude to Prof. Dr. Mohammad Arif Department of Geology, University of Peshawar for coming up with the idea and accompanied me to the field; however, due to unforeseen circumstances, I was unable to continue my thesis with him.

Second, I want to thank my supervisor Dr. Shahid Iqbal for taking me on as a student and overseeing everything. I also appreciate his critical evaluation of the thesis. That would not have been possible without his intelligent advice and conversation.

It is also appropriate to thank Prof. Dr. Mumtaz Muhammad Shah, Chairman Department of Earth Sciences, for his support and encouragement. Moreover, I would like to thank the staff and faculty of the Department of Earth Sciences for providing me with access to the resources and facilities necessary for this research. Their cooperation was crucial to the success of this project.

A special thanks goes out to my colleagues at the Geoscience Advance Research Labs Geological Survey of Pakistan Islamabad who assisted me in the lab and preparation of this study. Their support and company have been priceless.

Finally, I would like to thank my family and friends for their constant support and prayers throughout the years. Their love and belief in me have been the driving force behind my success.

TABLE OF CONTENTS

LIST OF FIGURES

List of Tables

ABSTRACT

Petrographic and geochemical features of alkaline rocks in the Michni area (Warsak), NW Pakistan, are being studied. Based on field relationships and petrographic observations, these rocks are classified as Pyroxenite, ijolite series rocks (melteigite-ijloite-urtite), Nepheline Syenite, Fenites and Carbonatite. So far, there have been no reports of Carbonatite in the study area. It has been reported for the first time. Ijolites predominate and have a wide variety of texture, with carbonatite intruding as well. Melteigite is found in close contact to ijolite. Pyroxenite was located along the metasediments. The remaining rocks are few and possibly eroded. A petrographic observation enabled the studied rocks to be classified into silica under-saturated rocks, that contain the essential minerals feldspathoids (nepheline that has primarily undergone cancrinite alteration), clinopyroxene, amphibole, carbonate, as well as accessories like titanite, apatite, garnet, carbonate, phlogopite, biotite, etc. whereas clinopyroxenes and amphiboles make up the majority of mafic rocks such as pyroxenites, melteigites and ijolites. Calciocarboantite is the chemical name for the carbonatite, which mostly comprises calcite. Fenitization linked with carbonatite results in altered rocks called fenites. Metasomatism of ijolitic or carbonatitic magma is most likely to be responsible.

CHAPTER 1
INTRODUCTION

Alkaline rocks are volumetrically insignificant and account for less than 1% of all igneous rocks. Despite this, their remarkable mineralogical diversity has brought them repeatedly to the attention of petrologists and mineralogists, with the result that alkaline rocks account for about half of all igneous rock names. There are 400 different varieties of alkaline rocks described by Sørensen (1974). This diversity is mostly the result of an excess of alkalis ($Na_2O + K_2O$) and a lack in silica, that together generate many mineral assemblages not stable in silica-rich, alkali poor magmas. Alkali pyroxenes, feldspathoids, and amphiboles are typical components of alkaline igneous rocks (Sørensen, 1974).

Alkaline silicate rocks mainly consist of pyroxenite, ijolite, and nepheline syenite that are closely associated with carbonatite either in individual complexes or in a regional association within magmatic provinces. The mineral assemblage is predominantly consisting of alkali feldspars, nepheline, cancrinite, sodalite etc., which are the characteristics of alkaline rocks. On the other hand, carbonatites are igneous rocks, occurring both as intrusive as well as extrusive bodies derived from mantle, although their origin is still controversial. They are having more than 50% carbonate (CO_3^{-2} bearing) minerals, and typically less than 10% SiO_2 (Wooleÿ and Kempe, 1989).

These rocks are usually characterized by very high concentrations of Light Rare Earth Elements (LREE) and other highly incompatible trace elements (e.g., Sr, Ba). Most of the world resources of Niobium (Nb), Tantalum (Ta) and other REE hosted in these rocks making them potential horizon strategically. Further, these are host to important radioactive elements (e.g., Th, U). The exigencies for these elements are continuously increased, particularly in industrial countries, thus carbonatite and associated rocks can be regarded as materials of the future (Kogarko et al., 2001). Pakistan is blessed with the presence of carbonatites and important outcrops of these rocks occur at Loe-Shilman, Sillai Patti, Jawar, and Jambil areas. Major exposures of the alkaline silicate rocks are located in Warsak, Shewa-Shahbazghari, Ambela, Tarbela and Malakand (Kempe and Jan, 1970; 1980). The study area has received little attention and could not properly addressed in the past. The detailed petrographic and geochemical study of the selected samples from Michni area has been done. In order to get rock classification, major mineral phases and tectonic setting of the area.

1.1 General Statement/Research Question/Hypothesis

The magmatic rocks of the Warsak area, NW Pakistan, are part of well-known Peshawar Plain Alkaline Igneous Province (PPAIP). Rocks comprising the PPAIP occur as isolated bodies of various dimensions scattered in the northwestern part of the Indian Plate in Pakistan. The occurrence of these rocks seems to be restricted to the region lying between the Main Mantle Thrust and the Main Boundary Thrust (Fig. 1.1). The PPAIP covers an area of about 1000 km^2 and extends for more than 150 km from the Pak-Afghan border in the west to Tarbela dam in the east. Its component rocks include alkali granites, porphyritic granites, quartz syenites, syenites, nepheline syenites, ijolites and carbonatites.

The origin of the PPAIP is still debated. According to Kempe and Jan (1970) and Jan et al. (1981a), Paleogene rifting led to the generation and emplacement of magma parental to the PPAIP. On the other hand, Le Bas et al. (1987), believe that rocks constituting the PPAIP formed in two widely separated alkaline magmatic episodes, i.e., Carboniferous and Oligocene, in which magmas were emplaced along thrust faults within and around the Peshawar Basin, rather than related to Paleogene rifting, i.e., Himalayan collision. In contrast to the above stated hypothesis, Butt (1989) and Jan and Karim (1990) proposed that all the rocks of the PPAIP were emplaced during Permo-Carboniferous. Khattak et al. (2005), supported the idea of Le Bas et al. (1987), that the alkaline and carbonatitic complexes with in the PPAIP occurred in at least two magmatic episodes, the Carboniferous and Oligocene.

The present research focuses on petrography and geochemistry of alkaline rocks. Carbonatites are often associated with alkaline silicate rocks but occurring without silicate rocks are also known worldwide as well as in Pakistan. It is important to note that carbonatite, which has not previously been reported, may be found in the study area. The detail sampling has done for classifying the rock units and tectonic setting of the area on the basis of petrography and geochemistry.

1.2 Aims And Objectives

Alkaline igneous rocks occur in the Michni area of Warsak, NW Pakistan. A detailed investigation of these rocks is planned aiming the following objectives:

1. Study field relationship of the Michni igneous body with the surrounding rocks to investigate its extent and distribution, and record its field and megascopic features.

2. Modal mineralogy determination, identification of constituent mineral phases, structural and textural characteristics.
3. Geochemical characterization of these rocks.
4. Determination of petrogenetic modeling and tectonic setting of the study area.
5. Comparison with the rest of magmatic rocks of PPAIP.

1.3 Methodology

Majority of the fresh samples were collected for petrographic and geochemical examination. Field relationships of the intrusion with the host rock were recorded and photographed. A total of 29 rock samples were collected based on textural variations ranging from intrusion, host and contact. These were then cut into thin sections for petrographic studies in Geoscience Advance Research Labs Geological Survey of Pakistan, Islamabad and studied under the Nikon petrographic microscope. Whereas 22 representative samples were selected from different rocks of the study area that were observed petrographically. These samples were ground for whole-rock geochemical studies in Geoscience Advance Research Labs Geological Survey of Pakistan, Islamabad. The whole-rock major elements analyses and trace element analyses have been obtained from X-ray fluorescence (XRF) technique. The detail about method of preparation and instrument will be discussed in the respective chapter.

1.4 Location And Accessibility

The Michni alkaline silicate complex at Shine Ghunda is exposed in District Mohmand of Khyber Pakhtunkhwa, was previously known Mohmand Agency and was a part of Federally Administered Tribal Areas (FATA). It is located 28 km northwest of Peshawar (34º 11′ 55″ N 71º 28′ 10″ E) & (34º 12′ 22″ N 71º 27′ 52″ E) spreading over the eastern side of Warsak and along the northern side of Kabul River. The elevation above sea level is 424 m. This is well accessible through Peshawar-Warsak Road and is also accessible from Charsadda-Shabqadar Road.

1.5 Climate

The climate in the study area is hot in summer season while cool in winter. The winter season starts from November and continue till February. The maximum temperature in summer is 38ºC while in winter minimum temperature is 12º C. The area experiences two rain seasons winter and summer but most of the rainfall is during winter season. Overall, the rainfall is insufficient. Water supply is from rainfall, snow melt and ground water during the dry periods.

1.6 Previous Work

Alkaline rocks in in the NW Pakistan were initially reported by Coulson (1936). He recognized aegirine, arfvedsonite in granitic samples collected by Sir Lewis Fermor from Khyber Agency and Shewa-Shehbazgarhi near Mardan. He published three analyses of the rocks and proposed that the rocks from the two localities resemble each other closely in composition. Ahmad (1951) investigated the acid granitic rocks from the Warsak region which are an extension of the same granitic bodies, sampled by Sir Lewis Fermor. Ahmad et al. (1969) and Martin et al. (1962) provided further information on the geology of Warsak (Khyber Agency) and Shewa-Shehbazgarhi areas respectively. Martin et al. (1962) included the rocks from Shewa-Shehbazgarhi area in their Shewa Formation, a small outcrop of soda-amphibole bearing rocks, which they named albite-porphyries. Siddiqui (1965) described a large granitic body about 3 km NE of Shewa-Shehbazgarhi. Besides granites, the complex contains nepheline syenites (Koga syenites), which tempted Siddiqui (1965) to propose a paragenetic linkage with alkaline quartzo-feldspathic rocks of Shewa-Shehbazgarhi. About two years later Siddiqui (1967) reported the occurrence of carbonatite bodies in association with the Koga syenites at the locality of Naranji Kandao and gave further account of the petrography of granites and syenites in the Ambela granitic complex. The occurrence of granitic rocks with alkaline affinities in Malakand was reported by Chaudhry et al. (1974, 1976). These alkaline granites having resemblance to the Warsak and Ambela granites based on their whole rock composition (Kempe, 1983), although they lack the typical alkaline minerals aegirine and riebeckite. Alkaline granites containing aegirine and riebeckite, are petrographically similar to the Warsak granites were also reported from the locality of Tarbela, SE of Shewa-Shehbazgarhi (Kempe and Jan, 1970). Tahirkheli et al., (1990) identified A-type nature of the Warsak granites. Rafiq et al. (2005) reported the eastern extension of Warsak alkaline rocks and named it Michni alkaline complex.

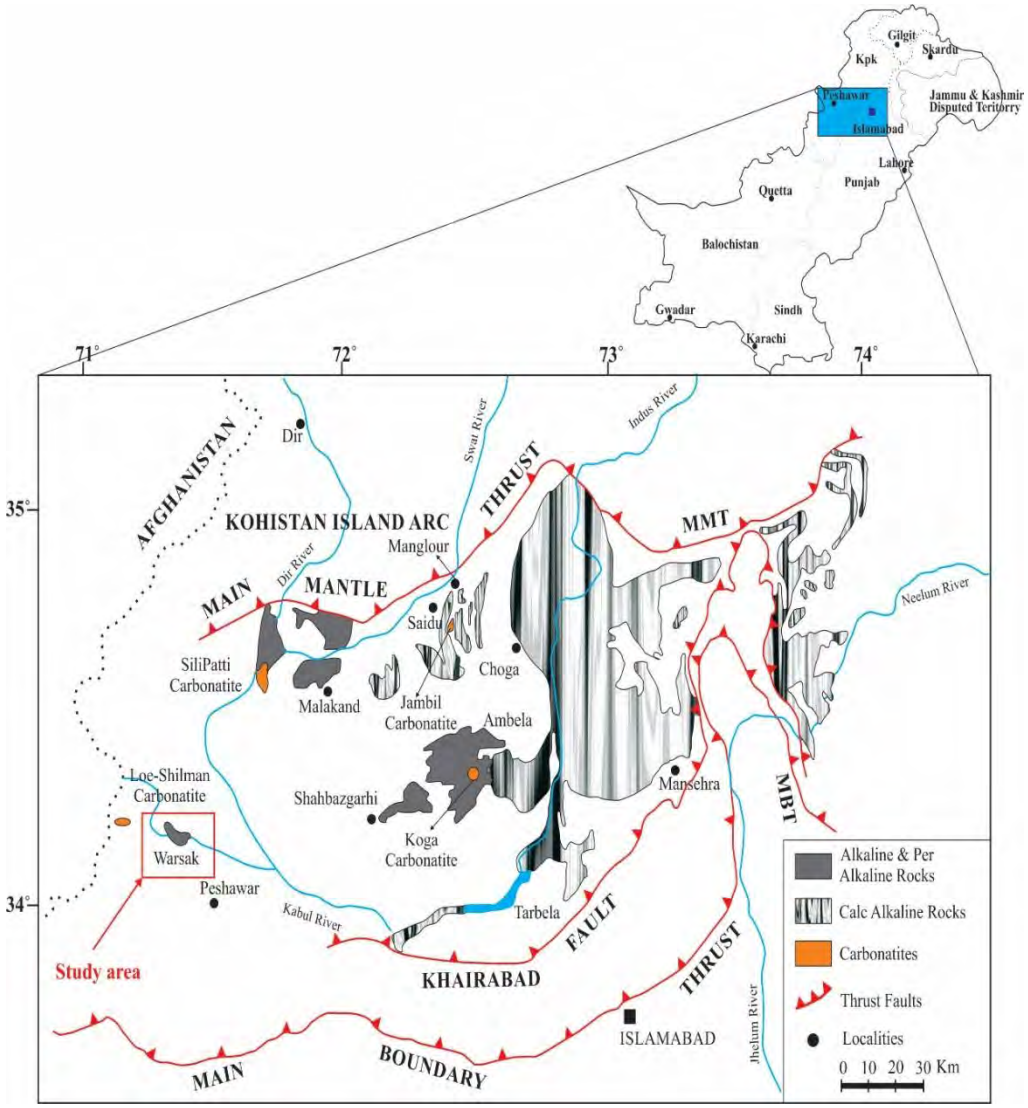

Figure 1.1. Map of the study area showing locations of alkaline rocks and carbonatites. Modified from Khattak et al., 2005.

CHAPTER 2

General Geology

This chapter includes the tectonic setting of northern Pakistan and major structures of the regional scale faults. In addition, the detail geology of the study area mainly emphasis on Peshawar Plain Alkaline Igneous Province (PPAIP) will be discussed.

2.1 Tectonic Setting

The Himalayan Orogeny is the result of Indo-Asian collision (Yin et al., 2000) when the Tethys oceanic realms that formed during the Paleozoic-Mesozoic due to the break-up of Pangaea into the Laurasia in the north and the Gondwana in the south, were eventually closed (Hsu et al., 1995; Sengör and Natal'in, 1996). Many crustal blocks of Eurasia comprised of various sizes sutured along ophiolite belts and several of these blocks were accreted to the Laurasia since the Carboniferous (Chang et al., 1973; Burrett, 1974; Sengör, 1984; 1988). Most of these were of Gondwanaland, which detached from the mother continent, drifted northward and successfully collided with the Laurasian Domain. The Present day Eurasia is thus comprised of the initial Laurasian landmass, the Laurasian domain, and the accreted assemblage of the former fragments of Gondwanaland. The Indian Plate rifted away from the Gondwanaland followed by the extensive seafloor spreading and opening of the Indian Ocean. The Indian Plate traveled northward and collided with Eurasia due to the subduction of the northern margin of the Indian Plate and resulted in the closure of the Neo-Tethys Ocean. The zone that marks the collision between the Indian Plate to the south and the Asian Plate to the north is called the Indus Tsangpo Suture Zone Gansser, (1980). This zone in the Western Himalayas separates the Kohistan-Ladakh Island Arc to the north from the Indian Plate to the south (Gansser, 1964; Bard, 1983), which is extending for >5000 km from southern Pakistan (near Karachi) to southern Burma (near Yangon) Gansser, (1980). After collision Kohistan-Ladakh Island arc complex evolved into a continental arc setting in the latest Cretaceous along the Shyok Suture Zone (Hodges, 2000), and was accreted to Asia between 102 ± 12 and ca. ~75 Ma (Petterson and Windley, 1985; Coward et al., 1987; Treloar et al., 1989).

The Kohistan Island Arc (KIA) is bounded to the north by Shyok suture or Main Karakoram Thrust (MKT) and to the south by Indus suture or Main Mantle Thrust (MMT). Tahirkheli et al., (1979) suggested that the entire Kohistan sequence represents the crust and

mantle of a complete island arc. Further work (Jan., 1980; Bard et al., 1980; Coward et al., 1982; Khan et al., 1998) supported the idea and that it is an obducted island arc turned on end during the Himalayan Orogeny. It consists of Late Cretaceous and Eocene plutonic belts, and pyroxene granulites, calc alkaline volcanics, amphibolites, and minor metasediments (Coward et al., 1984). It formed during the late Mesozoic by magmatism related to intra-oceanic subduction of the Tethys lithosphere. The KIA southward thrusting over the north Indian plate along the MMT probably took place in latest Cretaceous or Paleocene and was certainly completed by ca. ~ 55 Ma (Beck et al., 1995; Searle et al., 1999) (Fig. 2.1).

The Himalayan Range runs south of the Indus suture for >2000 km, between the Hazara–Nanga Parbat syntaxis in the west and the Namche-Barwa syntaxis in the east. Himalayan mountain belt has been subdivided into four structural domains separated by crustal-scale faults. The domains exactly correspond to four geographic domains as introduced by Gansser (1964). In Pakistan, the Himalayan division as it is in the east cannot be extended as such to the west. This is mainly for two main reasons. One is the amalgamation of the Kohistan Island Arc between India and Asia and the other is the lack of MCT in Pakistan. Therefore, only two out of four Himalayan divisions have been mapped in Pakistan. One is the Lesser Himalaya and the second is the Sub-Himalaya (Tahirkheli, 1982). In general, The Himalayan subdivision from north to south, include (Gansser, 1964, LeFort, 1975):

1. Tethyan or Tibetan Himalaya
2. Higher or Greater Himalaya
3. Lesser or Lower Himalaya
4. Sub-Himalaya

1.1.1 Tethyan Himalaya

The High Himalayas and its Central Crystalline Complex is bounded on the north by a northward dipping fault, the Trans-Himadri Fault (Valdiya, 1989). It is a Late Paleogene gravity collapse structure with several tens of kilometer movement (Burchfiel et al., 1985). North of this fault and overlying the Central Crystalline Complex there is a thick sequence of

Late Pre-Cambrian, Paleozoic and Mesozoic fossiliferous Tethyan sediments which was deposited on the northern passive continental margin of India (Thakur, 1981).

1.1.2 Sub-Himalaya

The Himalayan foothills form the Sub-Himalayan zone and from the Punjab to Assam these hills comprised of a narrow belt of folded Neogene molasse type sediments (Siwaliks). Northward the Main Boundary Thrust (MBT) terminates this sequence, which is the boundary between the Sub-Himalaya and the Lesser Himalayas (Heim & Gansser, 1939).

1.1.3 Lesser-Himalayas

This zone is bounded to the north by the Main Central Thrust (MCT) and to the south by Main Boundary Thrust (MBT).

1.1.4 High Himalayas

The Main Central Thrust forms the base of a huge 10-15 km thick slab of high-grade metamorphic rocks, which overlie the Lesser Himalaya sequence. This thrust sheet of Pre-Cambrian Central Crystalline from the High Himalaya and the very core of the Himalayan range.

Each of these tectonostratigraphic zones is separated from the another by crustal scale thrusts or normal faults (Le Fort, 1975 and references there in). These structures record squeezing of the northern margin of the Indian Plate since Eocene collision which according to Coward and Butler (1985) is 470 km and according to Coward et al., (1988), is more than 730 kms. In the above context, the carbonatites and associated alkaline rocks are restricted in the region lying between MMT in the north and MBT in the south.

2.2 Major Structures

The major structures are separated by parallel regional scale faults from north to south as discussed below in detail:

1. South Tibetan Detachment System (STDS) It is a major structure and connects low-grade metamorphic rocks of Tibetan Himalaya over high-grade metamorphic rocks of Greater Himalaya and also mark the southern limit of the Tibetan Himalaya.

2. MMT Indus suture narrows substantially and continues westward the suture referred as MMT. It was identified as the continuation of the Indus suture zone by Tahirkheli et al., (1979). It separates the

Kohistan Island Arc to the north from the Indian Plate to the south (Gansser, 1964; Bard, 1983), and marks the entire southern and eastern boundaries of the Kohistan Island Arc (DiPietro et al., 2000). MMT was described as extending eastward from Afghanistan through Swat to Babusar and then northward around the Nanga Parbat-Haramosh massif to Ladakh where it relates to the Indus suture zone (DiPietro et al., 2000). In Pakistan, the MMT has been reactivated as a N-dipping normal fault, causing the unroofing of high-grade metamorphic rocks (Anczkiewicz et al., 2001).

3. Main Central Thrust (MCT) (it marks the southern limit of Higher Himalaya). MCT is located to the south of MMT or Indus Suture Zone. It is the intra crustal thrust formed as a result of collision between the Indo-Asian plates during Oligocene (Heim & Gansser, 1939). In the north Pakistan, the presence of the MCT is limited and arguable (Coward et al., 1988; Chaudhry and Ghazanfar, 1990; DiPietro et al., 1999).

   The Panjal Thrust (Khairabad Fault) has been considered as an analogue of Main Central Thrust (MCT) in Kashmir and NW Himalaya. Lefort (1986), considered the Main Boundary Thrust (MBT) and Panjal Thrust to represent the subsurface extension of MCT.

4. Main Boundary Thrust (MBT) (it marks the southern limit of Lesser Himalaya). The MBT separates the foreland basin deposits which were produced by up lift and subsequent erosion of the Himalayas and deposited by rivers. These rocks have been folded and faulted to produce the Siwalik Hills that are at the foot of great mountains.

5. Main Frontal Thrust (MFT) (it marks the southern limit of Sub-Himalaya). The MFT is a surface expression of a low-angle, basal thrust or the Himalayan Sole Thrust that demarcates the southernmost extent of the foreland basin fold and thrust belt along which it has been thrusted over sediments on the Indian Plate. MFT represents the toe of the Himalayan orogenic wedge (Hodges, 2000).

The three distinct domains are present in northern Pakistan from north to south comprising of (i) the Eurasian Plate, (ii) the Kohistan Island Arc, and (iii) Indian Plate. The study area is the part of Indian Plate constituting PPAIP and lies in Pakistan. It contains several igneous complexes of mildly to strongly alkaline character. The igneous complexes include Loe-Shilman carbonatite complex, the Warsak alkaline granites, the Sillai Patti carbonatite complex, the Malakand granite, the Shewa-Shahbazgarhi complex, and the Tarbela alkaline complex which was defined as Peshawar Plain Alkaline Igneous Province (PPAIP) by Kempe and Jan (1970; 1980).

The alkaline and carbonatitic magmatism occurred in two distinct episodes in northern Pakistan: one during the Carboniferous and the other in the Oligocene. The Warsak alkaline

granites, Malakand granite, Shewa-Shahbazgarhi complex, Ambela granitic complex and Tarbela alkaline complex were emplaced during the Carboniferous magmatic episode, while the Loe-Shilman and Sillai Patti carbonatite complexes were emplaced during Oligocene magmatic episode (Le Bas et al., 1987; Qureshi et al., 1990; Khattak et al., 2001). Khattak et al., (2005 & 2008) also supported the occurrence of Oligocene alkaline magmatic episode in the region.

The study area, which was described as the eastern extension of Warsak alkaline rocks intrudes metasedimentary rocks of Marghazar Formation. Its age is early Paleozoic that hosts the alkaline magmatism in the area. The metasedimentary rocks consist mainly of slates, quartzite, phyllites, schists and marbles that have some characteristics of green schist facies. While the intrusion is made up of a variety of rocks, from feldspathoidal syenites to alkali-syenites, melteigites, ijolite, and mica-pyroxenite.

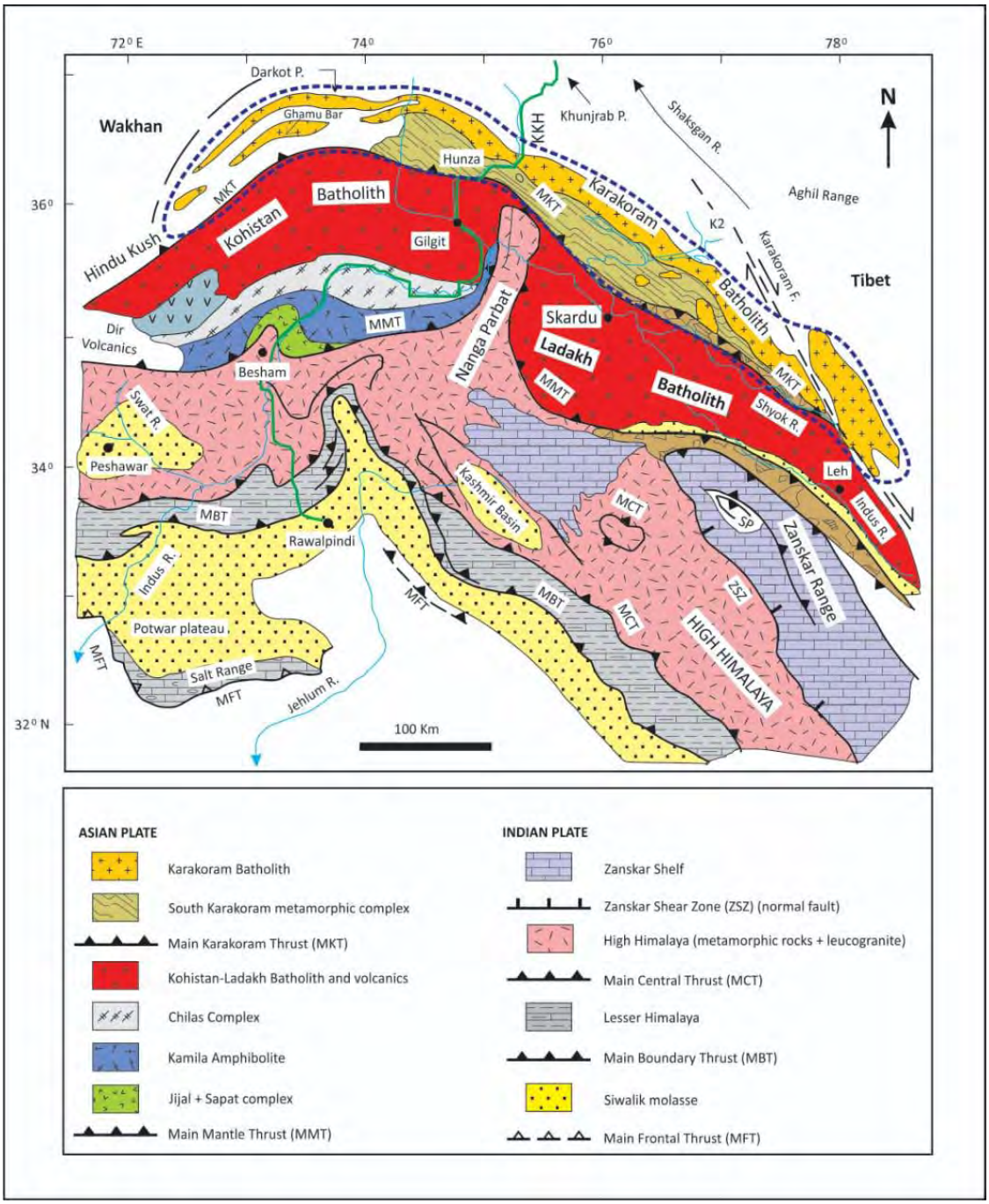

Figure 2.1. Tectonic map of Northern Pakistan (redrawn from Searle et al., 1999; Searle & Trelaor, 2010).

CHAPTER 3

DATA SETS

This chapter is comprised of detailed petrographic studies in order to obtain modal mineralogy and textural relationships within the rocks. This chapter also contains geochemical data from the studied rock samples.

3.1. FIELD OBSERVATION

The isolated intrusive body of Michni (Warsak) is a composite intrusion into the Paleozoic metasediments (Fig. 3.1). A sharp northern contact with the metasediments is exposed while the rest contacts are not exposed and mostly covered with alluvium. The intrusion is composed of variety of ultramafic-alkaline silicate and carbonatite rocks. During the fieldwork, 29 samples were collected. These samples were cut into thin sections for detailed petrographic studies.

The study outcrop is very limited in area (< 2 km^2) and is highly heterogenous. The intrusion is dominated by ijolites associated with pyroxenite (Fig. 3.2). Ijolite shows a large textural variation from fine to coarse grained and carbonatite intruded in the ijolite as well (Fig. 3.3). The carbonatite is coarse grained and deeply weathered. The carbonatite is not reported from the study area so far. Melteigite rock occur as sharp contact with ijolite (Fig. 3.4). This is composed of fine to medium melanocratic rock. Within the Melteigite veins of alkali feldspar also occur. The nepheline syenite occurs as smaller body in the intrusion. In addition, leucocratic rock which is fine to medium also observed. The pyroxenite is micaceous and occurs at the contact with metasediments; within the pyroxenites, amphibole rich pyroxenite also exists and malachite staining was also seen (Figs. 3.5 3.6).

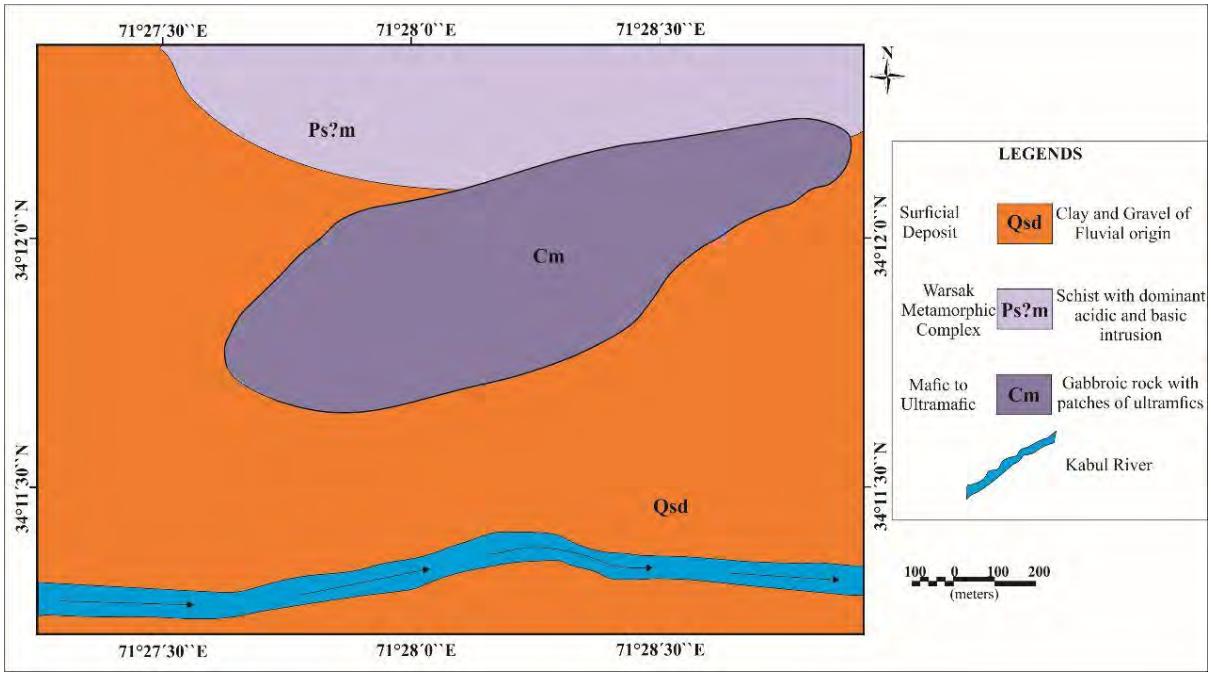

Figure 3.1. Geological Map of the study area (after Khan et al., 1995).

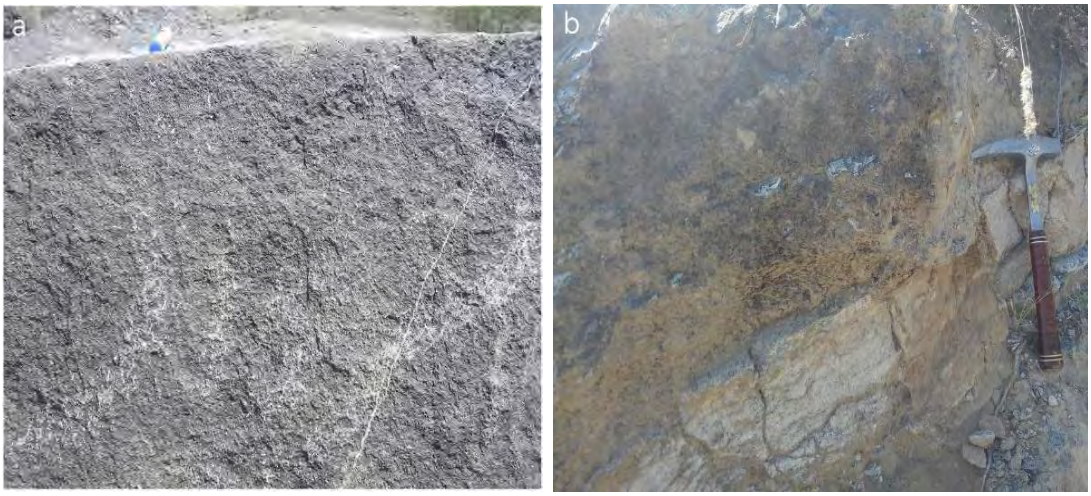

Figure 3.2. Field photographs of the Michni area (a) pyroxenite (b) carbonatite intruded in ijolite. Hammer for scale length 13 inches.

Figure 3.3. Field photographs of the Michni area (c) A sharp contact between Ijolite and Melteigite (d) Alkali feldspar veins in Melteigite.

Figure 3.4. Field photographs of the Michni area (e) coarse grained Ijolite. (f) Malachite staining observed.

Figure 3.5. Field photograph of micaceous pyroxenite in the Michni area.

3.2 PETROGRAPHIC OBSERVATION

3.2.1. Pyroxenite (samples S-13, S-22, S-26, S-28 and S-29)

Pyroxenites are composed of 80-90 % clinopyroxene, 0-10 % amphibole 3-5 % apatite and various accessory phases (titanite, nepheline, phlogopite and carbonate). The modal abundance of various minerals is shown in the Table. 3.1. Clinopyroxene in sample S-29 shows oscillatory zoning from colorless core to light green rims while the rest has irregular and patchy zoning (Fig. 3.6). Clinopyroxene is anhedral to subhedral, elongated grains of augite (lighter green) while in other samples the clinopyroxene is aegirine-augite. Longer amphibole occurs along the margins and thus encloses clinopyroxene (sample S-22). In addition, titanite is overgrown by garnet and amphibole occurs as rims overgrown on titanite. Titanite also called Sphene, titanium and calcium silicate mineral, $CaTiSiO_4$ (O, OH, F). The mineral titanite contains titanium, which is the ninth most abundant element in the earth's crust and is common accessory mineral of plutonic igneous and metamorphic rocks. Single grain titanite encloses clinopyroxene and apatite. The grains of nepheline are relatively small present (sample S-28) that is altered along the rims to cancrinite. Nepheline is frequently altered into the secondary phase cancrinite, a member of the feldspathoid group of minerals. Its chemical formula is $Na_6Ca_2(AlSiO_4)_6(CO_3)_2.2(H_2O)$ which is an aluminosilicate and contains sodium and calcium. Small apatite crystals are included in and larger apatite forming an interlocking pattern with clinopyroxene. Carbonate is interstitial and fracture filling that is most likely calcite but has not been investigated. In sample S-29 the titanite is interstitial, the phlogopite has also been observed in this sample.

3.2.2. Amphibole-rich pyroxenite (sample S-10)

This rock is mainly composed of amphibole (67 %), cancrinite (12-15 %), epidote and clinopyroxene (8 %), and accessories include titanite, apatite, and garnet (Fig. 3.6). Epidote is a characteristic of metamorphic rock; however, it also occurs as a result of hydrothermal alteration (Howie et al., 1992). It most likely happens as a clinopyroxene alteration in the study area. The amphibole is long prismatic dispersed throughout the thin section associated with a small amount of clinopyroxene. Clinopyroxene contains inclusion of phlogopite and apatite. Cancrinite and epidote occur as anhedral grains, cancrinite is first order gray to yellow interference colors. Epidote containing inclusions of apatite and opaque ore. Anhedral titanite and garnet are also observed.

3.2.3. Melteigite (Samples S-1, S-6, S-7 And S-30)

Melteigites show a wide range of modal variations and are composed of clinopyroxene (55-80 %), altered and nepheline (10-20 %), alkali feldspar (20 %) and perhaps other minerals include (10-20 %). Among them are apatite, titanite, carbonate, phlogopite, biotite, garnet, sodalite, ore, amphibole, plagioclase and fluorite. All melteigites are fine to medium grained. Clinopyroxene (sample S-1) shows regular oscillatory-zoned from colorless core to lighter green rims, while clinopyroxene from the other samples shows irregular and patchy zoning (Fig 3.6). Clinopyroxene is anhedral as the grain size increases. Larger (a few mm locally) and interstitial amphibole has been observed along the rims of clinopyroxene showing alteration product of clinopyroxene. One sample (S-30) has larger grains (~ 1mm) of augite up to 60 % and nepheline containing inclusion of clinopyroxene and phlogopite. The rest of the samples have altered nepheline (cancrinite) anhedral to subhedral grains with yellow to gray first order interference colors and some have high interference colors. The larger grains of potassium feldspar are perthitic. The anhedral to subhedral crystals of titanites are dispersed throughout the thin section (Fig. 3.7). The anhedral apatite crystals form an interlocking pattern with clinopyroxene, and smaller crystals are found as inclusions in clinopyroxene with titanite. Twinning is observed in both clinopyroxene and titanite. Carbonate is present as interstitial. Sodalite and phlogopite occur in this rock type (Fig. 3.8).

3.2.4. Ijolite (Samples S-2, S-3, S-11, S-12, S-17 And S-23)

Ijolites are composed of clinopyroxene (40–45 %), nepheline altered and unaltered (50–55 %) and accessory include titanite, apatite, cancrinite, and carbonate. The ijolites vary in texture from coarse to fine on hand specimen. Clinopyroxenes (aegirine-augite) have been observed in all samples and are included in nepheline and cancrinite. Clinopyroxenes are scattered throughout the section in the groundmass of nepheline (altered and unaltered), but typically clinopyroxene is locally large (~ 1mm) anhedral to subhedral in habit and shows irregular and patchy zoning and some have oscillatory zoning, from yellow cores to bright green rims (Fig. 3.6). Twinning is also observed in clinopyroxene. Anhedral biotite is present at the rims of clinopyroxene. Amphibole is present in sample S-23 commonly in association with clinopyroxene and partly replaces it. Nepheline is altered to its typical alteration product cancrinite that is first order grey to high interference colors in samples S-2, S-3, and S-17, which is euhedral to subhedral in small or larger grains. In remaining samples nepheline is relatively fresh and only become altered toward cancrinite along the rims and fractures. Titanite and garnet are found in both types (i.e., overgrowth and single grains). Titanite is

found intergrown with and included in garnet. In samples S-2 and S-3 titanite intergrown with garnet are abundant and constitute 8-10 % of the rock. Apatite is commonly found in the shape of needles and bamboo as an inclusion in nepheline and clinopyroxene. Carbonate is an interstitial mineral that is commonly found with garnet and titanite.

3.2.5. Urtite (Samples S-5, S-19 And S-21)

Urtites are composed of altered and unaltered nepheline (75-80 %), clinopyroxene (5-20 %) and amphibole (10 %) as major constituent. Titanite, apatite, garnet, carbonate, phlogopite, biotite and alkali feldspar are some of the accessories. Nepheline grains are euhedral to subhedral often altered to cancrinite, which occur along the grain boundaries and crack filling. Cancrinite is first order grey, and some have high interference colors. One sample (S-19) contains fine grained altered anhedral nepheline (cancrinite) in addition this sample has overgrowth of different minerals such as apatite, carbonate, and probably cancrinite on garnet together with clinopyroxene and titanite. Single crystals of euhedral titanite also occur. Clinopyroxene is anhedral to subhedral showing regular zoned from colorless core to darker yellow rims, amphibole occurs along the rims of clinopyroxene. Apatite needles like included in and form interlocking pattern with clinopyroxene and other minerals. Carbonate, phlogopite, biotite have been found in trace amounts. Carbonate can be found as interstitial or as small single grains.

3.2.6. Fenites (Sample S-8 And S-9)

Fenites are altered rocks produced by fenitization associated with carbonatite. It is most likely caused by metasomatism of ijolitic or carbonatitic magma. The fenite is composed of potassium feldspar (50-65 %) cancrinite (10-30 %) and plagioclase (0-25 %) and accessories include clinopyroxene, sodalite, carbonate replacement, biotite and phlogopite. The potassium feldspar is perthitic and the grains are subhedral to anhedral surrounded by cancrinite with a small amount of fresh nepheline and laths of plagioclase. Apatite included in nepheline and clinopyroxene and also as single crystals. Carbonate appears as an interstitial and fracture filling. Because of the abundance of potassium feldspar, these rocks are known as potassic fenites. Furthermore, potassic fenites form in the presence of sövitic carbonatites (Le Bas, 2008).

3.2.7. Nepheline Syenite (Sample S-16, S-18 And S-27)

The major constituents of nepheline syenite are altered and unaltered nepheline (50-65 %), potassium feldspar (15-20 %), clinopyroxene (10-15 %), and plagioclase (20 %). The remaining 5% is composed of titanite, apatite, phlogopite, carbonate, and opaque ore. Nepheline is anhedral to subhedral, which altered to gray to yellow colors cancrinite along grain boundaries and fractures. Nepheline encloses the grains of clinopyroxene, potassium feldspar, apatite and phlogopite. Clinopyroxene is large subhedral to anhedral scattered throughout the rock. Titanite and phlogopite generally occur as rims overgrown on clinopyroxene, single crystals of titanite may also observe. Potassium feldspar is perthitic and laths of plagioclase showing carlsbad twinning. Titanite and apatite are both present in clinopyroxene and nepheline. Carbonate is found as a secondary mineral. In sample 18MJ clinopyroxene 20 %, altered and unaltered nepheline 25-45 % potassium feldspar and plagioclase 5-10 %. Apatite, titanite, phlogopite, and biotite are present in trace amounts. Nepheline is subhedral to anhedral containing inclusion of apatite, titanite and phlogopite and potassium feldspar. Titanite and biotite both occur as single grains and overgrowth on clinopyroxene.

3.2.8. Carbonatite (Sample S-4)

Carbonatite has a coarse-grained white sugary texture, is highly weathered, and occurs as veinlets in the field. It is white on fresh surface while dark grey on weathered surface observed along the roadside. It is intruded into the ijolite and is considered to be the youngest phase of the intrusion. Its maximum thickness is 2 meter and less than 1-meter-wide dipping roughly towards the north.

The carbonatites are geochemically classified as sövite type. Microscopically it is mostly composed of euhedral to subhedral carbonate grains >90 % (Fig. 3.8). Apatite, biotite, zircon and opaque are present in accessories.

Table 3.1 Modal mineralogical composition of studied rocks. Nep. Nepheline Canc. Cancrinite Alkf. Alkali Feldspar A.A. Aegirine Augite Plg. Plagioclase Carb. Carbonate Carb Rep. Carbonate Replacement Amp. Amphibole Sph. Sphene Grt. Garnet Sod. Sodalite Ore. Opaq

	Nep	Canc	Alkf	A-A	Plg	Carb	Carb Rep	Amp	Sph	Apt	Grt	Sod	Ore	Bt	Epdt	Flrt
S-1	--	20.9	9.3	50.1	--	2.3	--	--	6.1	2.7	2.4	4	1.9	--	--	--
S-1A	--	--	>80	--	--	--	--	--	--	--	--	--	--	--	--	--
S-2	--	39.4	--	40.5	--	1.7	10.8	--	--	2.4	7.2	--	1.5	--	--	--
S-3	--	56	--	43	--	--	--	--	--	--	--	--	--	--	--	--
S-4						>90										
S-5	70.5	4.7	0.8	21.2	--	--	--	--	--	1.4	1	--	--	0.1	--	--
S-6	--	6.5	18	65.6	0.5	--	3.3	3.2	1.5	0.3	--	--	--	--	--	--
S-7	11.3	--	--	79.6	--	--	0.4	7.7	--	0.7	--	--	--	0.03	--	--
S-8	1.1	29.5	67.5	--	--	--	--	--	--	--	--	--	--	1.6	--	--
S-9	--	12.1	49.5	2	25.8	--	5.5	--	--	--	--	5	--	--	--	--
S-10	--	12.3	--	7.7	--	--	--	67	1.7	0.6	2.2	--	--	--	8.5	--
S-11	48.8	1.8	0.3	46.3	--	--	--	--	0.8	0.9	1	--	--	--	--	0.1
S-12	50	1	5	40	--	--	--	--	2	1	1	--	--	1	--	--
S-13				>90												
S-16	35	15	15	15	20	--	--	--	--	--	--	--	--	--	--	--
S-17	0.8	40.7	--	47	5.1	--	--	--	2.4	0.3	3.3	--	--	0.07	--	--
S-18	25	43	5	20	7	--	--	--	--	--	--	--	--	--	--	--
S-19	--	78.8	0.6	16.4	0.5	1.1	--	--	1.3	0.8	--	--	--	--	--	--
S-20	--	12	25	30	10	12	--	--	--	2	--	--	--	8	--	--
S-21	59.5	15.7	--	4.5	--	--	--	9.4	5.14	1.8	3.7	--	--	--	--	--
S-22	--	--	--	80	--	--	--	10	5	5	--	--	--	--	--	--

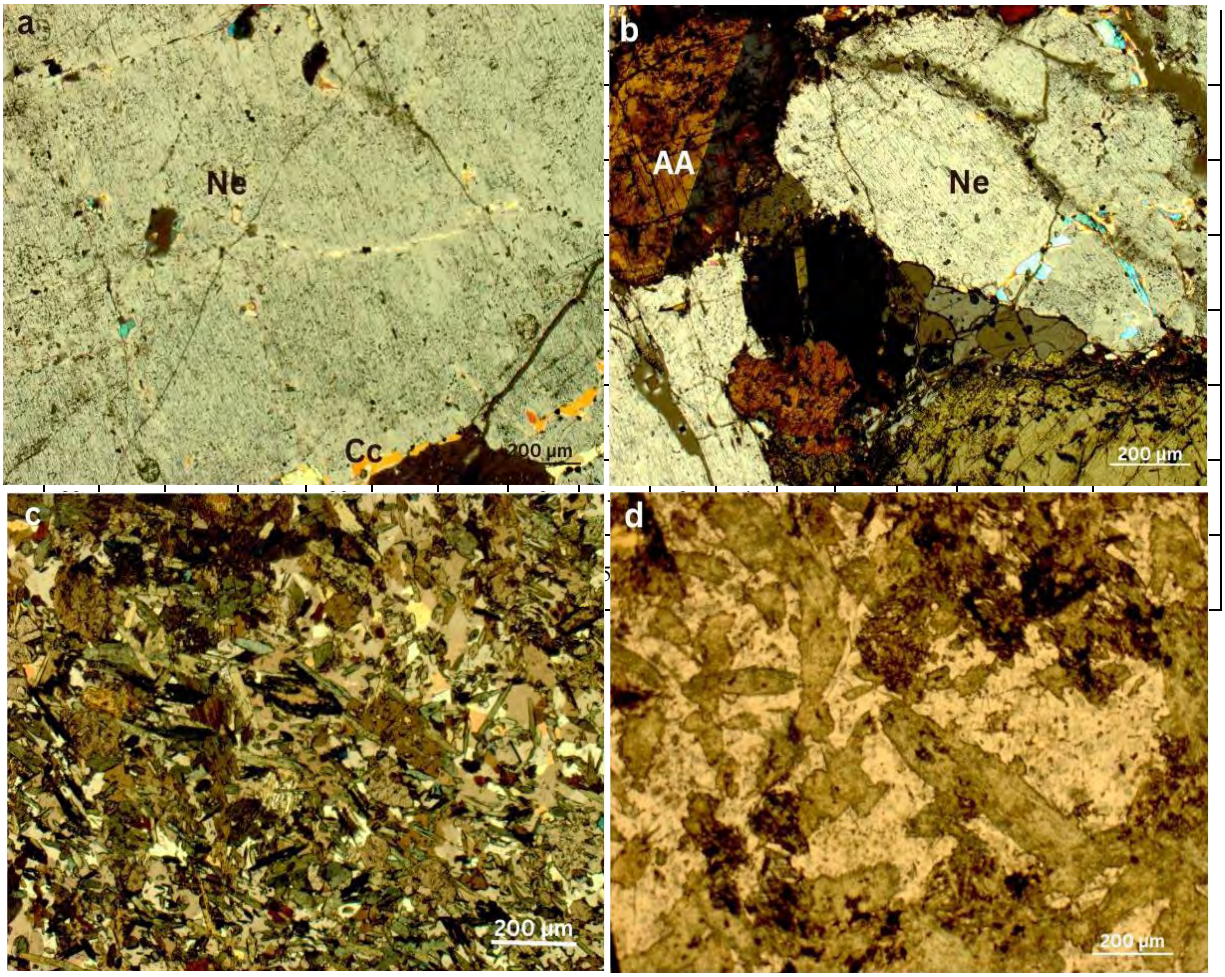

Fig. 3.6. Photomicrographs of the Michni area (a) Nepheline and altered Cancrinite. (b) Nepheline, Aegerine Augite, Cancrinite. Patchy zoning in Aegerine Augite. (c) Ne=nepheline Cc=cancrinite AA=aegirine augite

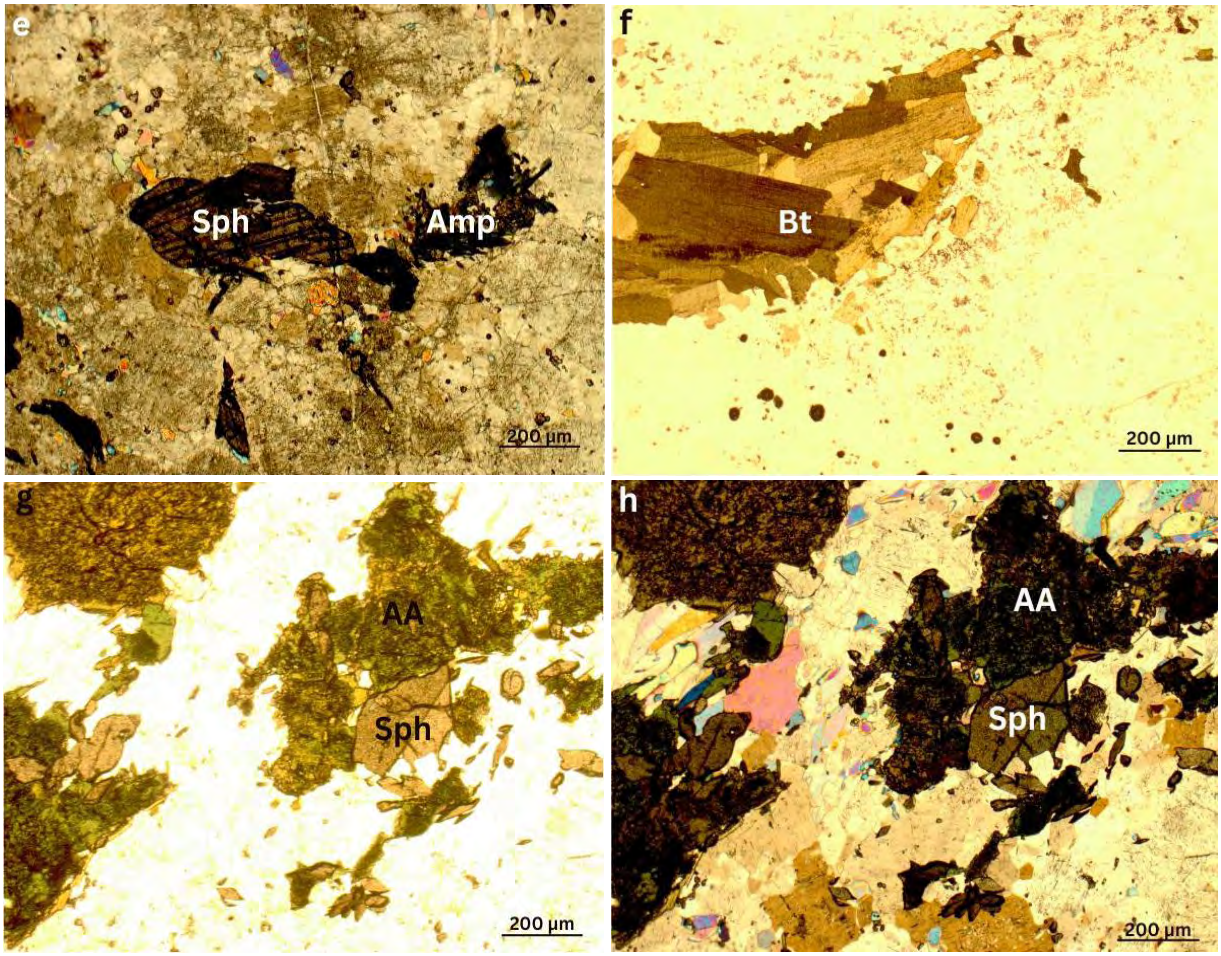

Fig. 3.7. Photomicrographs of the Michni area (e) Sphene and Amphibole. (f) Biotite. (g) Aegerine Augite and Sphene in PPL. (h) Aegerine Augite, Sphene, Nepheline and Cancrinite in XPL. Sph=sphene Amp=amphibole Bt=biotite AA=aegerine augite

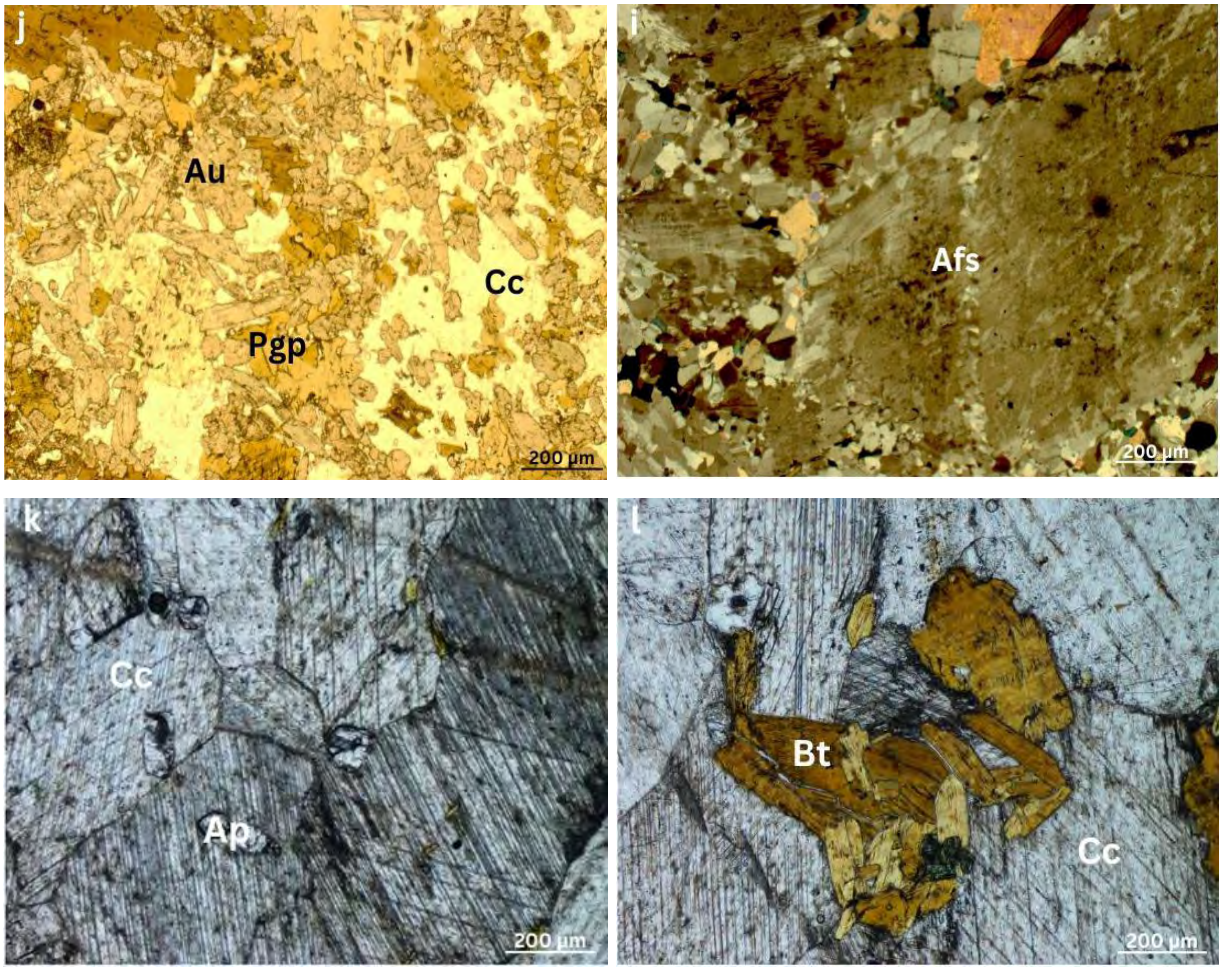

Fig. 3.8. Photomicrographs of the Michni area (i) Perthitic Alklali Feldspar. Microfractures in the perthite grains contain fine-grained alkali feldspar. (j) Augite, Phlogopite with intermittent Cancrinite. (k) Carbonatite having coarse grained calcite and apatite in PPL. (l) Carbonatite having Biotite in PPL. Afs=alkali feldspar. Au=Augite Pgp=Phlogopite Cc=cancrinite. Cc=calcite Ap=apatite. Bt =biotite.

3.3. Geochemistry

The analyzed rocks underwent geochemical analysis to determine the whole-rock major oxide content in weight percent and the trace element concentration in ppm. The details are shown below.

3.3.1 Methodology

The total no of 22 representative samples were ground for whole-rock geochemical studies in Geoscience Advance Research Labs Geological Survey of Pakistan, Islamabad. The major elements analysis and trace element analyses have been obtained using X-ray fluorescence (XRF) technique. Each sample was crushed in a a c rusher and then pulveri ed in a tungsten carbide ball mill to ca. 200 mesh si e. or ma or element o ides ca. 5 g of each sample a s dried overnight at 110 ºC for removing moisture and then kept in a muffle furnace at 950 ºC for two hours to obtain loss on ignition (LOI). After placing in desiccator for cooling and then 0.7 g of sample was mixed with 3.5 g of lithium tetraborate flux. To make it bead equal amount of weight loss was added to 3.5 g. The sample-flux mixture was fused in platinum-gold crucible at 1100 ºC for 25 minutes. A few drops of releasing agent lithium iodide were added to the mixture. During this period the crucible was periodically swirled over a burner to eliminate the gas bubbles and ensure the thorough mixing and homogeneity of the melt. The melt was cast between aluminum discs and left there for some time. Major elements were measured from the fusion discs along with standard using RIGAKU XRF-3370E spectrometer. The detection limits for major elements are as follows: SiO_2 (0.27%), TiO_2 (0.014%), Al_2O_3 (0.13%), Fe_2O_3 (0.08%), MnO (0.005%), MgO (0.03%), CaO (0.09%), Na_2O (0.02%), K_2O (0.03%), and P_2O_5 (0.03%). The trace element analysis of the samples were performed on powdered pellets, and the detection limits for the majority of trace elements are roughly 0.1-1 ppm. An approximately 12 gm of powdered dried samples was mixed with 3 gm of wax with the help of a small glass rod. Placing mixture in a steel cup to become a shape of pellets by applying pressure. The powdered pellets were placed in XRF spectrometer for the analyses of the following set of elements: Sc, V, Cu, Cr, Ni, Zn, Ga, As, Br, Rb, Sr, Y, Zr, Nb, Mo, Ag, Cd, Sn, Ba, La, Ce, Hf, Pb, Bi, Th. The concentrations of major elements are given in weight percent (wt %) of oxides and trace elements are reported in parts per million (ppm).

3.3.2. Major Elements Geochemistry

The representative whole-rock major and trace element concentration are listed in Tables 3.2 3.3 and 3.4. The carbonatite has very low quantities of SiO_2, Al_2O_3, Fe_2O_3, total alkalis, and P_2O_5 and includes CO_2 42.76 and 42 weight percent, CaO 48 and 51 weight percent. Loss on ignition is used to determine volatiles. The studied rocks are of alkaline nature distinguished petrographically but chemically also observed as alkaline in a plot of total alkalis versus silica diagram. Most of them are strongly alkaline except Pyroxenite which has low total alkalis thus fall in subalkaline field and anomalously enriched in MgO suggesting clinopyroxene fractionation. Furthermore, these rocks are metaluminous (mol. $Na_2O+K_2O < Al_2O_3$) and characterized Aluminum Saturation Index < 1.0 according to Shand, 1943 showing calcic phases such as Amphibole and Pyroxene in the studied rock as also revealed in petrographic studies. The Nepheline Syenite of the studied sample is miaskitic character. The agpaitic index [$((Na_2O+K_2O)/Al_2O_3)$ molar] has a narrow range varies from (0.42–0.71) and reflects the miaskitic mineralogy. However, the fact that alkaline rocks include both silica-saturated and silica-undersaturated rocks that may be either peralkaline or metaluminous phases (Frost et al., 2008). The mineralogical composition of the studied rocks visible in Harker variation plots suggested evolution through fractional crystallization. These include alkali feldspar, amphibole, pyroxene, biotite, sphene and apatite fractionation.

3.3.3. Trace Elements Geochemistry

Abundance of several trace elements in studied rocks are plotted against primitive-mantle normalized multi element pattern are presented in different Figures. This is the fact that these rocks contain rare accessories concentrating in most trace elements usually in Th, U, Zr, Hf, Nb, Ta etc. Carbonatite sample shows distinct trends. It is enriched in trace elements relative to primitive mantle as general enrichment in Sr (4156.3 ppm) and Ba (476.3 ppm) in comparison to rest of the elements. Ti and Yb are depleted while the rest elements are enriched in comparison to primitive mantle. The contents of numerous trace elements are almost similar in Pyroxenite and Melteigites except Ba, Nb, Zr and Pb are higher in concentration in Ijolite in comparison to Pyroxenite. The Ijolite samples are somewhat enriched in Ba, Nb and Pb whereas depleted in Sr, Ti and Zr. The Urtite and Fenite showing enrichment in U and Pb making peaks except one sample and Sr, Zr, Nb showing moderate concentration. The Nepheline Syenite is characterized by enrichment in Rb, Ba, K and Pb whereas moderate in Th, U, Nb, Sr and low in Zr, Y. The concentration Nb, Zr, Ba, U, Th are usually considered as indications of the presence of REEs in the studied rocks.

Table 3.2. Representative major and trace elements whole-rock analyses of the study area.

Rock type	Carbonatite	Pyroxenite				Melteigite			
Sample no.	**4**	**13**	**22**	**28**	**29**	**1**	**6**	**7**	**30**
SiO_2	4.10	56.60	54.13	52.76	54.91	45.23	50.00	45.21	41.67
TiO_2	0.19	0.70	0.93	0.62	0.62	1.81	1.14	0.51	1.20
Al_2O_3	0.27	6.93	6.32	4.97	3.12	9.56	8.42	12.20	12.13
Fe_2O_3	1.36	8.64	8.02	6.98	6.81	10.45	12.34	10.87	11.30
MnO	0.40	0.21	0.19	0.17	0.13	0.19	0.28	0.25	0.24
MgO	0.00	2.67	1.32	2.34	3.40	2.67	3.12	2.35	3.23
CaO	48.12	20.34	23.10	26.90	25.83	17.45	15.01	14.98	16.25
Na_2O	0.34	1.56	1.87	1.56	1.15	7.28	4.19	6.98	8.34
K_2O	0.55	0.57	0.44	0.33	0.47	0.60	0.33	0.31	4.47
P_2O_5	0.08	0.01	0.65	0.75	0.58	0.32	0.42	0.50	0.29
L.O.I.	42.76	0.75	2.05	0.75	0.55	2.85	3.15	3.90	0.60
Total	**98.16**	**98.98**	**99.02**	**98.14**	**97.58**	**98.41**	**98.40**	**98.06**	**99.73**
Sc	45.5	71.5	9.9	50.1	74.3	19.8	28.7	20.8	25.2
V	2	150.2	95.7	220.4	151.2	217.5	200.6	127.9	331.2
Cr	8.8	110.1	10.9	74.5	131.5	51.7	41.8	34.1	89.5
Co	6.7	46.1	22	38.4	38.5	52.6	35.6	28.6	39.2
Ni	LLD	33.8	6.7	16.5	28.7	7.7	26.4	10.9	21.9
Cu	2.4	84.2	3.4	1.6	294.5	484.8	210.8	5.2	138.3
Zn	10.7	43.2	28.2	44.9	34.5	66.5	53.2	46.9	96.9
Ga	11.9	14.1	9.1	3.3	3.1	8.5	13.9	4.8	12.2
Rb	35.8	7.9	59.7	5.2	16.4	9.4	7.9	13.9	99.9
Sr	4156.3	214.4	282.3	572.7	281.8	374.6	415.3	547.1	289.1
Y	80.3	5.9	11.1	28.7	13.9	34.8	21.7	22.6	21.9
Zr	LLD	58.4	30.9	45.8	36.1	171.9	97.3	143.3	92.2
Nb	LLD	2.6	6.5	2.3	1.8	64.2	39	15.8	21.8
Mo	0.3	0.1	LLD	0.1	LLD	2.6	LLD	0.1	0.1
Sn	0.1	LLD	0.5	0.6	LLD	1.1	LLD	6.8	1.6
Sb	40.1	8.5	2	15.5	12.8	7.6	7.1	2	5.7
Cs	11.2	LLD	LLD	15.5	LLD	4.7	0.6	LLD	6.4
Ba	476.3	181.8	231.4	66.9	215.5	65.2	710.6	1125.6	1315.7
La	43.5	16.8	18.7	48.4	25.4	31.7	27.1	21.9	41
Ce	82.9	LLD	16.1	92.9	35	41.2	33.4	18.5	42.4
Nd	53.7	4	3.1	46.2	28.9	41.9	13	15.8	17.2
Sm	LLD	LLD	LLD	10.3	LLD	4.1	LLD	LLD	LLD
Yb	0.2	LLD	LLD	LLD	LLD	1.2	2.2	LLD	LLD
Hf	9.8	9.2	6	8.1	7	9.4	13.1	6.4	3.6
Ta	4.5	LLD	LLD	2.2	LLD	LLD	7.9	LLD	LLD
W	318.4	266.5	244.3	121.5	125.2	359	312.3	154.2	125.8
Pb	11.4	1.5	1.8	3.5	7.7	96.2	33.2	12.1	5.1
Bi	1.1	LLD	LLD	0.1	LLD	0.9	1.4	LLD	0
Th	1.9	1.4	2	5.1	3.3	8.4	2.1	4.9	4
U	29.2	0.1	1.9	3.2	0.7	3.4	2.3	2.6	1.1

Table 3.3. Representative major and trace elements whole-rock analyses of the study area.

Rock type	Ijolite						Urtite	
Sample no.	2	3	11	12	17	23	19	21
SiO_2	45.97	46.20	47.23	48.56	49.34	44.54	60.14	58.98
TiO_2	1.04	1.61	0.96	0.40	1.01	0.81	0.36	0.83
Al_2O_3	15.89	17.34	17.12	18.84	19.12	17.24	12.32	14.16
Fe_2O_3	8.47	9.13	8.02	6.97	7.69	7.78	5.43	4.65
MnO	0.23	0.22	0.22	0.14	0.25	0.16	0.09	0.06
MgO	0.90	0.89	0.08	0.00	0.00	0.00	0.00	0.00
CaO	15.56	14.04	13.98	9.12	7.98	12.67	7.34	6.40
Na_2O	6.63	7.29	7.18	8.79	8.12	9.66	9.98	8.98
K_2O	0.28	0.43	2.57	3.83	4.62	0.93	1.34	2.89
P_2O_5	0.46	0.22	0.43	0.26	0.09	0.14	0.03	0.03
L.O.I.	3.75	2.75	1.30	1.10	1.20	4.90	1.55	2.95
Total	**99.17**	**100.12**	**99.09**	**98.01**	**99.42**	**98.83**	**98.58**	**99.94**
Sc	25.4	18	25	9.9	3.5	13.5	0.5	1.9
V	297.1	284.9	224	95.7	102.8	144.2	51.3	67.5
Cr	80.8	50.8	51.2	10.9	14.8	19.7	2.9	6.7
Co	30.8	47.2	37.4	22	28.2	21.6	16.2	38.9
Ni	3.5	6.6	14.4	6.7	0.8	7.4	2.3	4.3
Cu	197	888.6	246.9	3.4	LLD	56.1	0.3	23.8
Zn	75.4	128.4	41.1	28.2	123.7	36.2	17.7	20.5
Ga	12	10	8.3	9.1	18	3.8	20.5	8.7
Rb	9.5	15	35.6	59.7	89.6	28.9	3	37.2
Sr	546.8	383.9	353.1	282.3	534.1	1028.7	178.4	316.6
Y	64.6	65.3	16.2	11.1	28.3	10.3	6.2	11.7
Zr	158.1	199.4	50.9	30.9	173	54.9	101.7	34.5
Nb	25.6	19.8	13.8	6.5	39.1	25.9	25.2	52.3
Mo	1.1	1.1	LL D	LLD	LLD	LLD	0.4	0.5
Sn	1.9	LLD	0	0.5	LLD	15.3	8.2	4.3
Sb	12.1	8.4	7.6	2	0.9	2.1	0.6	1.6
Cs	LLD	LLD	LL D	LLD	LLD	LLD	LLD	LLD
Ba	25.3	71.1	381.5	231.4	891.9	5978.4	100.1	1099.9
La	41.9	24.6	27.7	18.7	35.1	12.5	15.1	14.9
Ce	67.4	33.3	37.5	16.1	22.4	3.1	4.8	24.6
Nd	28.6	29	23.7	3.1	11.8	LLD	5.1	LLD
Sm	LLD	2.3	LL D	LLD	LLD	LLD	LLD	LLD
Yb	LLD	2.1	LL D	LLD	2.2	LLD	LLD	LLD
Hf	3.4	2.8	2.5	6	0.8	6.3	LLD	3.7
Ta	LLD	LLD	LL D	LLD	1.6	7.1	LLD	8.3
W	437.7	300.8	432.9	244.3	327.4	120.3	240	233
Pb	30.6	3.1	3.7	1.8	5.4	7.7	LLD	0.8
Bi	0.6	0.4	LL D	LLD	LLD	LLD	0.2	LLD
Th	7.6	6.3	2.9	2	11.2	1.3	1.3	2.1
U	3.2	2.9	2.5	1.9	4.6	4.7	0.1	2.1

Table 3.4. Representative major and trace elements whole-rock analyses of the study area.

Rock type	Fenites		Nepheline Syenite		
Sample no.	**8**	**9**	**16**	**18**	**27**
SiO_2	56.12	55.23	58.02	58.01	57.56
TiO_2	0.21	0.38	0.25	0.40	1.01
Al_2O_3	23.12	19.34	20.56	21.01	17.45
Fe_2O_3	3.38	4.16	3.87	2.56	5.66
MnO	0.08	0.22	0.10	0.08	0.12
MgO	0.00	0.00	0.00	0.00	0.00
CaO	0.00	6.97	0.00	0.00	4.67
Na_2O	9.23	7.74	9.12	11.40	8.34
K_2O	2.52	0.38	5.27	3.45	3.63
P_2O_5	0.15	0.44	0.01	0.01	0.03
L.O.I.	2.95	4.45	0.40	1.05	0.90
Total	**97.75**	**99.29**	**97.59**	**97.98**	**99.37**
Sc	3.6	10.9	0.6	0.5	2.4
V	36.9	64.6	11.4	12.2	130.8
Cr	8.2	33.3	4	15.4	9.1
Co	17.4	24	16.3	13.3	32.8
Ni	2.2	8.4	1.6	2.4	2
Cu	54.4	3.5	2.5	0.6	323.2
Zn	40.5	34.5	37.9	32.6	28.5
Ga	8.9	13.2	16.1	19.9	15
Rb	63.1	14.2	103.2	62.3	43.9
Sr	434.6	592.5	340.5	279.9	267.4
Y	10.6	44.6	6.5	7.6	12.7
Zr	86.2	81.6	84.6	134.6	58.2
Nb	26.7	39.8	10.2	14.6	43.5
Mo	0.7	LLD	0.4	LLD	LLD
Sn	8.9	5.7	4.9	9	3.6
Sb	5.5	3.9	1	0.9	LLD
Cs	LLD	LLD	LLD	0.2	LLD
Ba	2773.6	392.6	626.9	703.3	108.6
La	13.3	19.4	8.9	8.9	17.4
Ce	4.9	41	1.9	9.8	14.2
Nd	LLD	39	6.5	0.4	9.9
Sm	LLD	LLD	LLD	LLD	LLD
Yb	LLD	6.1	LLD	LLD	LLD
Hf	8.4	6.4	0	4.4	3
Ta	LLD	2.7	0.8	3.2	2.6
W	179.6	276.6	287.6	304	282.7
Pb	23.5	4.6	3.3	0.1	6.3
Bi	LLD	LLD	LLD	LLD	0.1
Th	3.7	4.6	3	1.3	2.4
U	14.6	2.7	0.5	0.7	1.3

CHAPTER 4

INTERPRETATION AND DISCUSSION

This chapter includes the interpretation of results followed by comparing and significance of prior studies. The preceding chapter shows the concentrations of whole-rock and trace element data. The Geochemical Data Toolkit GCDkit is used to geochemically depicts these rocks on different diagrams (Janouek et al. 2006). The petrographic and geochemical studies of the magmatic rocks of Michni (Warsak) area are the main objectives of the present study. The results from these studies are used to reveal the petrogenetic and tectonic setting of the area.

4.1 Petrographic and Geochemical Features

Before incorporating the petrographical and geochemical, it is important to examine field relationship between the different rock types of observation are:

1. Ijolite is the dominant rock type and shows discordant relationship with pyroxenite
2. Pyroxenite is the oldest rock type.
3. Carbonatite intrudes in ijolite and shows sharp contacts.

These field observations indicate that pyroxenite is earliest phase of crystallization and so on the rest of rock crystallized. Carbonatite is the youngest unit.

The petrographic studies revealed that the rocks identified are mineralogically different assemblages especially in modal mineralogy and texture. These magmatic rocks can be grouped into carbonatite and alkaline silicate rocks. The alkaline silicate rocks include (Pyroxenite, Melteigite, Ijolite, Urtite, Fenite, and Nepheline Syenite). The rocks appear strongly undersaturated with respect to silica as demonstrated by the presence of feldspathoid minerals such as nepheline, cancrinite and sodalite. Carbonatite is identified as calciocarbonatite typical sövite which has coarse-grained interlocking calcite grains (Fig. 4.1).

Fenite is a metasomatic alteration product developed around carbonatite and associated silicate rocks. Fenitization is the process of alteration generally result from multiple pulses of alkali-rich fluid expelled from cooling and crystallizing carbonatitic or alkaline melt (Morogan, 1994; Le Bas, 2008; Elliott et al., 2015). They are typically composed of alkali

feldspar, albite, pyroxene and amphibole (Table 4.1) (Zharikov, 2007). The identified Fenite is potassic type which is mainly developed around sövitic carbonatite (Le Bas, 2008) and the presence of phlogopite in the rocks further evidence of potassic metasomatism in the study area (Holub et al., 2010). In addition, the abundance of secondary minerals and replacement textures suggests that the process of alteration is due to the activity of metasomatism in the studied rocks. These secondary minerals include are cancrinite, carbonate, amphibole, epidote, chlorite, phlogopite. In some rocks there is presence of felspar rich veins observed optically also provide support of metasomatism in the study area.

Cancrinite is also produced as a result of secondary mineral assemblages replacing primary magmatic minerals due to metasomatic reactions and hydrothermal alteration (Mariano, 1983; Chakhmouradian and Mitchell, 2002; Marks et al., 2003; Graser and Markl, 2008; Schilling et al., 2009; Borst et al., 2016; Elliott et al., 2018). These hydrothermal fluids result in the formation of the minerals in fenite and miaskites (Rass et al., 2006). Brecciation, a byproduct of the fluids and volatiles of the magma in a carbonatite or alkaline complex , is also noticeable in the study area (Elliott et al., 2018).

According to geochemical characteristics, the carbonatite in the study area is of the calcic type, which is equivalent to the sövite (typically with over 90 % calcite) Verwoerd (1967), and contain 48 and 51 wt. % CaO, 42.76 and 42 wt. % CO_2; and very low SiO_2, Al_2O_3, Fe_2O_3, total alkalis and P_2O_5 contents; and is typical calciocarbonatite (Woolley and Kempe, 1989) classificatory diagram (Fig. 4.1) similarly, to what we said in the paragraph before. As well as a plot of total alkalis vs silica diagram showing that the analyzed rocks are alkaline in nature and can be differentiated by petrography as well as chemically supports this in (Fig. 4.2). Most of them are strongly alkaline except Pyroxenite which has low total alkalis thus fall in subalkaline field and anomalously enriched in MgO suggesting clinopyroxene fractionation. Furthermore, these rocks are metaluminous (mol. $Na_2O+K_2O < Al_2O_3$) and characterized Aluminum Saturation Index < 1.0 according to Shand, 1943 showing calcic phases such as Amphibole and Pyroxene in the studied rock as also revealed in petrographic studies in (Fig. 4.3).

These rocks have rather considerable differences in the concentrations of the majority of the main oxides, but only minor variations in the silica content. Due to the relatively small range of SiO_2 content in the Michni rocks, the Harker diagrams on (Fig. 4.4) are of limited value for defining differentiation trends revealed by chemical analyses of these rocks. Additionally,

there is little to no evidence provided by the Harker diagrams for the fractionation of constituent minerals leading to the derivation of Michni rocks from a common parental magma.

The Nepheline Syenite of the studied sample is miaskitic character. The agpaitic index [($(Na_2O+K_2O)/Al_2O_3$) molar] has a narrow range varies from (0.42–0.71) and reflects the miaskitic mineralogy. However, the fact that alkaline rocks include both silica-saturated and silica-undersaturated rocks that may be either peralkaline or metaluminous phases (Frost et al., 2008). The mineralogical composition of the studied rocks visible in Harker variation plots suggested evolution through fractional crystallization. These include alkali feldspar, amphibole, pyroxene, biotite, sphene and apatite fractionation in (Fig. 4.5).

Primordial mantle normalized multi-element patterns for the studied rocks are shown in Figs. 4.5, 4.6 and 4.7. All samples indicate enrichment in the plotted elements in comparison to the undifferentiated primordial mantle (McDonough et al., 1992). These rocks are distinguished by extremely wide variations in the concentrations of the majority of trace elements. This is explained by the presence of rare accessories concentrated in Th, U, Zr, Hf, Nb, Ta, and other elements. The higher concentrations of Th, Ta, and Nb, which is most likely the result of pyrochlore (niobium) crystallization (Srivastava et al. 2005) although pyrochlore was not observed optically. The instrument's ability to detect Ta is normally low of the studied samples but the concentration that has already been identified is encouraging.

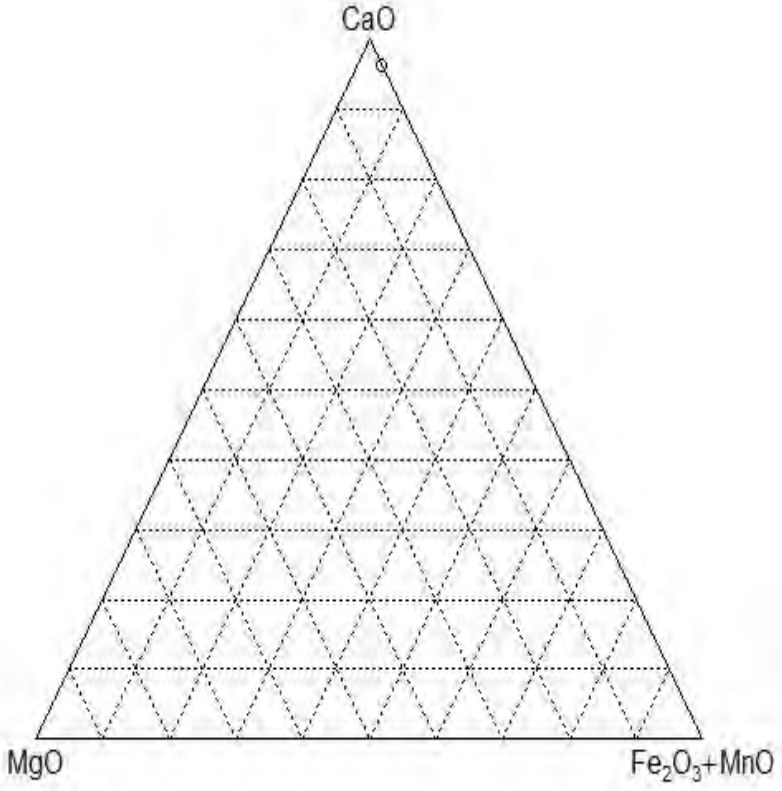

Figure 4.1. Carbonatite ternary CaO – MgO – (Fe2O3 + MnO) discrimination diagram after Woolley and Kempe (1989). The carbonatite plots in the field of calciocarbonatite. Fe2O3= total iron. Symbol of Carbonatite sample.

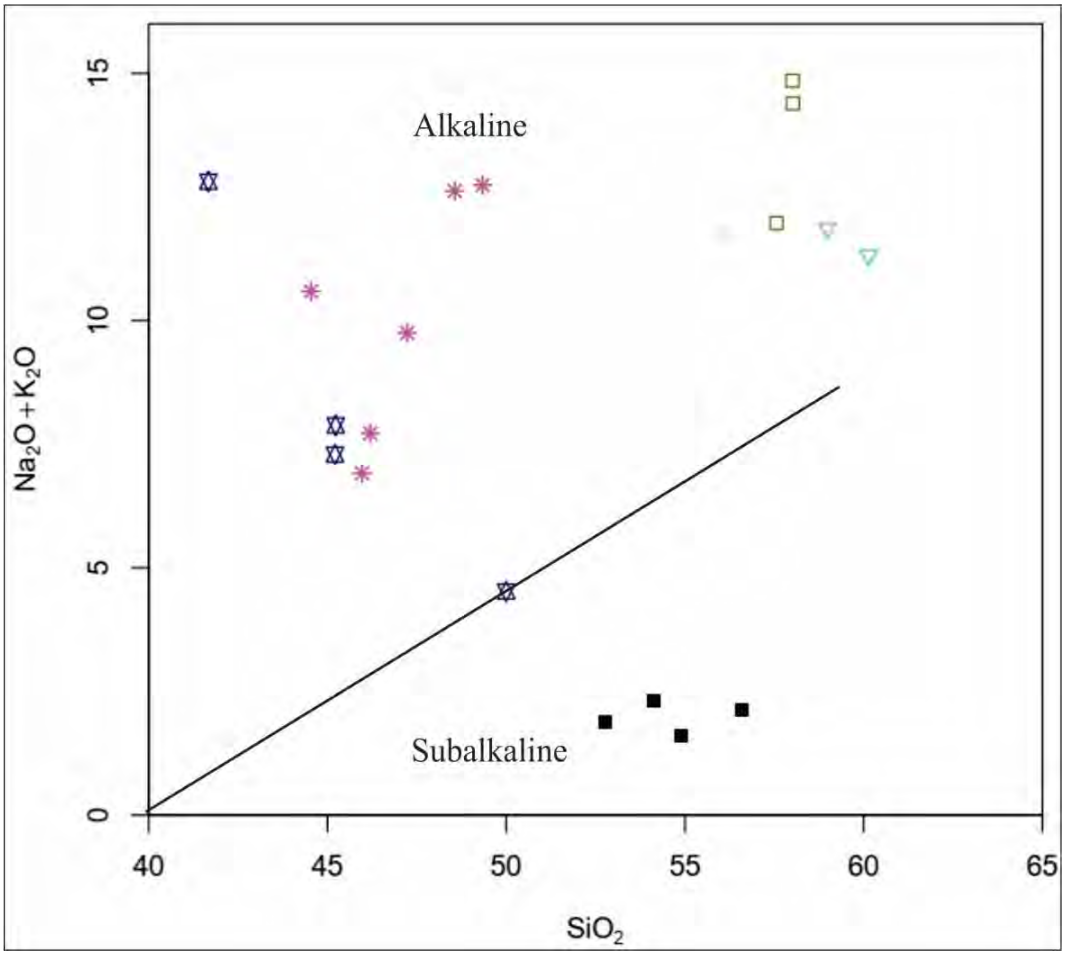

Figure 4.2. A plot of total alkalis versus silica. Symbols are the same as in Fig. 4.3.

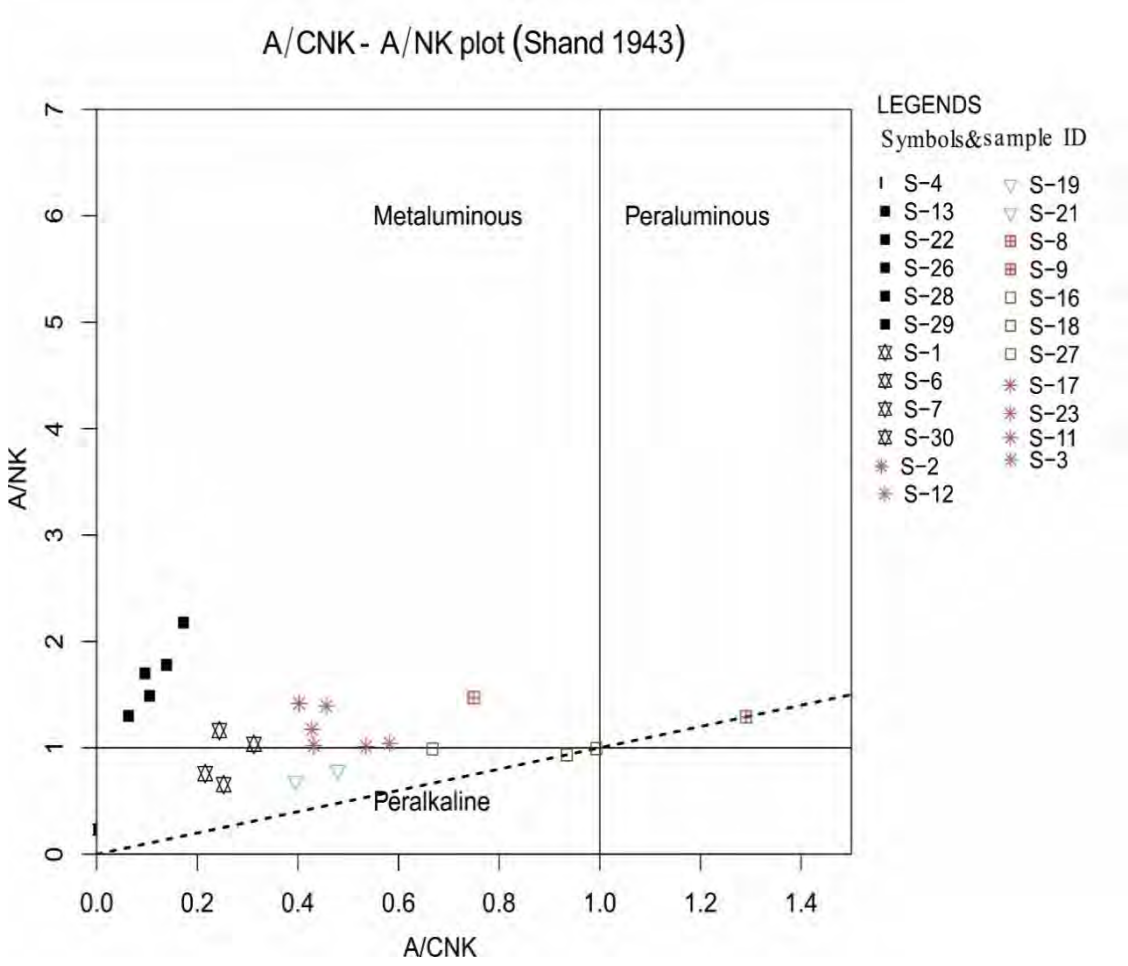

Figure 4.3. A/CNK v. A/NK diagram for the studied rocks. Symbols of the studied rocks (Shand 1943).

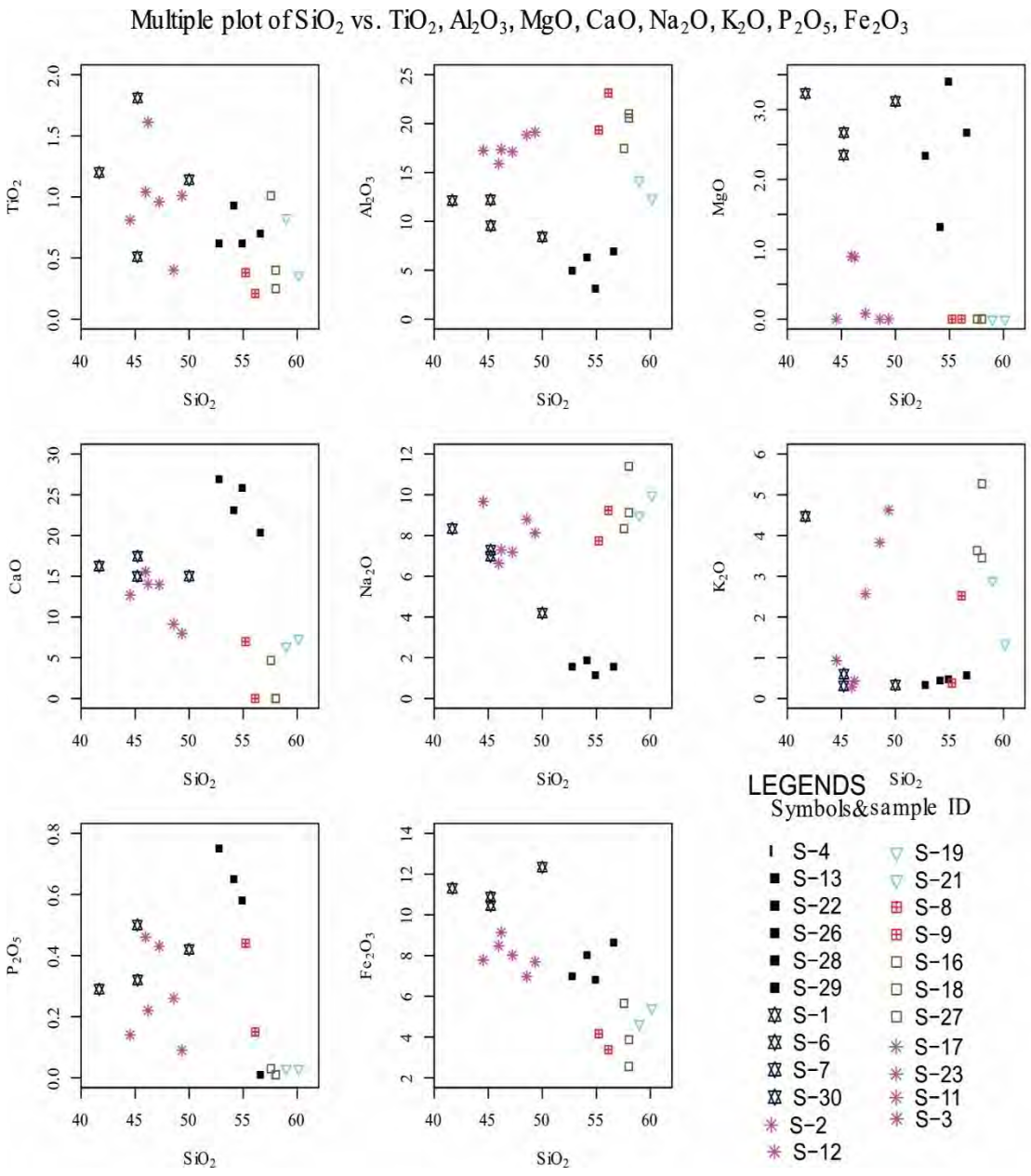

Figure 4.4. Major element oxides versus silica variation diagram Harker

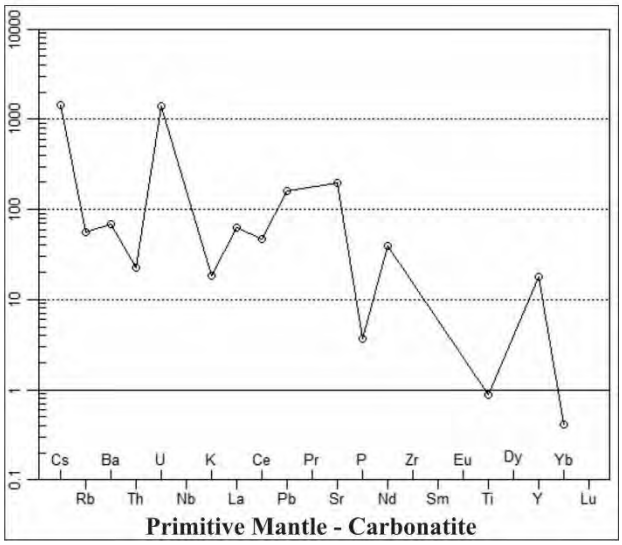

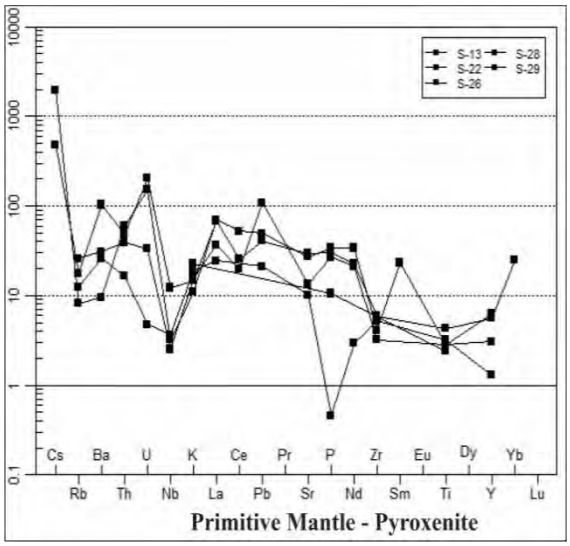

Figure 4.5. Primitive mantle normalized multi-element spider diagrams for Carbonatite and Pyroxenite (McDonough et al., 1992).

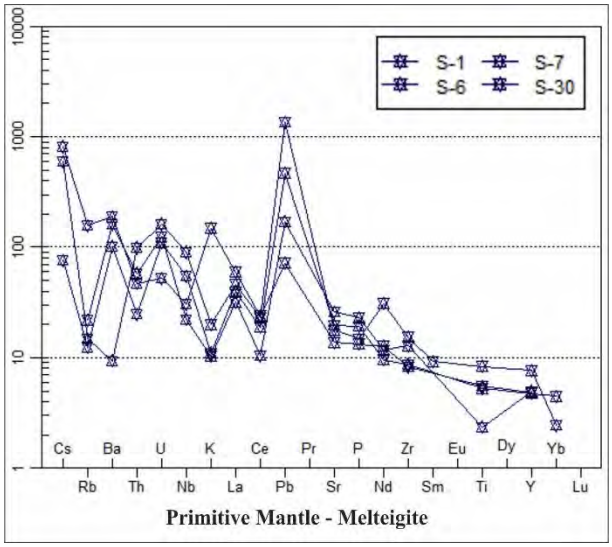

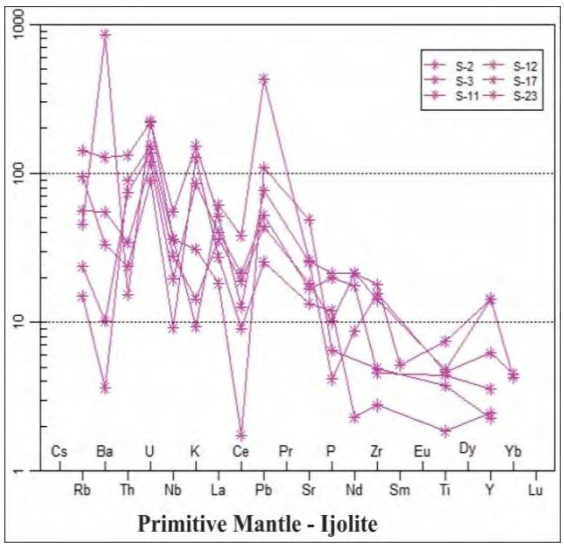

Figure 4.5. Primitive mantle normalized multi-element spider diagrams for Melteigite and Ijolite (McDonough et al., 1992).

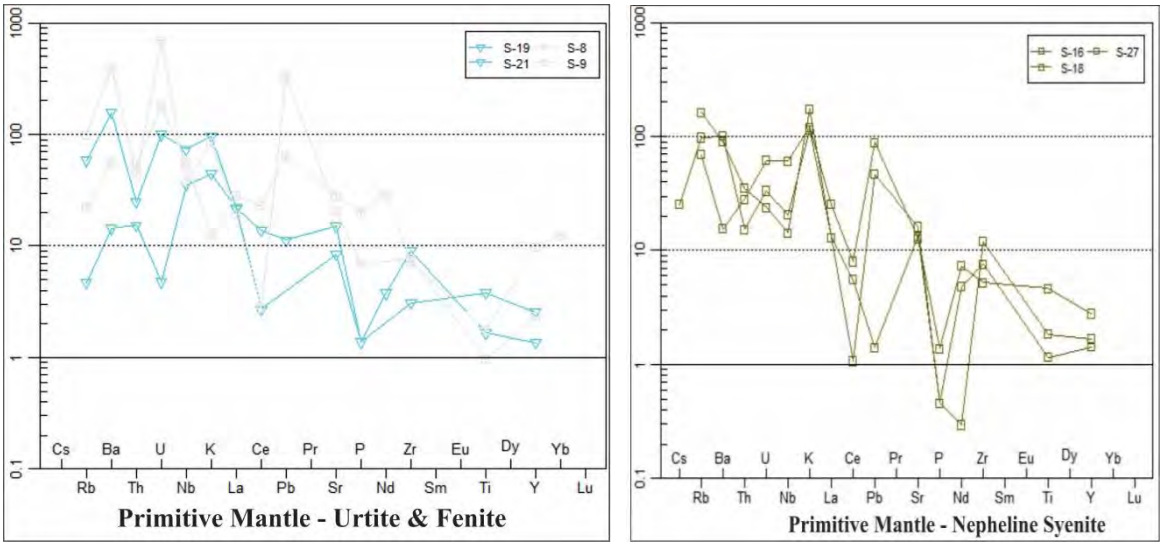

Figure 4.6. Primitive mantle normalized multi-element spider diagrams for Urtite, Fenite and Nepheline syenite (McDonough et al., 1992).

Geochemical and petrographic examinations have been used to try to identify any genetic relationships between carbonatite and silicate rocks, but the most effective method for doing so is isotopic analysis. Nepheline Syenite and carbonatite have completely different geochemical properties than the Ijolite and Pyroxenites. Similar pattern elements and genetic relationships can be seen in both pyroxenite and ijolite (Srivastava et al., 2005). Even with these rocks, there are certain geochemical differences that are hard to explain if they all originated from the same magma chamber, though. It is clear that whereas silicate rocks are made from various melting, they all originate from the same place. The most distinct geochemical patterns and chemical composition can be seen in carbonatite samples. Therefore, it is likely that the carbonatites came from a unique distinct magma.

4.2 Comparison with the same rocks as in the study area

According to (Rafiq and Jan, 1989), the Ambela Granitic complex, which is the primary component of the alkaline complex and is made-up of silica-saturated and undersaturated rocks which is composed of granite alkali granite, quartz syenite, alkali quartz syenite, syenite, alakli syenite, feldspathoidal syenites, ijolites, carabonatites and related rocks of Koga area. These rocks are lithologically similar to the rocks of the present research. In addition, they hypothesized that the alkaline rocks in the Ambela region are with-in plate and rift related, suggesting that major rifting occurred during the late Paleozoic disintegration of the northern Gondwana. Similar to the study area, a sövite plug 500 m across is entirely covered by a 50 m thick layer of K-feldspar rock near Koga in Buner (Le Bas, 1987).

4.3 Emplacement of studied rocks

The alkaline and carboantite rocks are thought to have been formed during episodic magmatism. Le Bas 1987 came to the conclusion that PPAIP was unrelated to the Himalayan collision because carbonatite complexes lack evidence of rifting. Additionally, he comes to the conclusion that the alkaline rocks and associated carbonatite of north Pakistan were emplaced during the Tertiary (Oligocene) and Carboniferous magmatic episodes. He further divided PPAIP into two groups: Permo-Carboniferous (which included Carbonatites and Koga Nepheline Syenites), and Mid Tertiary (Loe-Shilman and Sillai Patti carbonatites).

Khattak et al., 2012 presented two ideas on the emplacement of carbonatite in PPAIPs i) along a thrust fault in the compressional regime, and ii) along a rift zone of normal faulting. The Koga Carbonatite is carboniferous and conforms to normal intraplate magmatisam (Le Bas 1987). As a result, the resemblance of the lithology to this study strongly supports that it

was occurred during intraplate magmatism during the Carboniferous era. Generally, many researchers have proposed different theories that are still unclear.

4.4 Tectonic setting

The trace element data is further plotted on various discriminant diagrams to investigate a probable tectonic setting of the studied rocks using granite tectonic discrimination by Pearce et al., 1984. Rb v. Y + B and Nb v. Y (Fig. 4.8) reveal that the studied rocks show transitional behavior belong to both within in plate and volcanic arc syn-collisional settings. However, the examined samples show a higher degree of alteration, making classification difficult. Additionally, the majority of the sample suggests transitional behavior as a result of alteration.

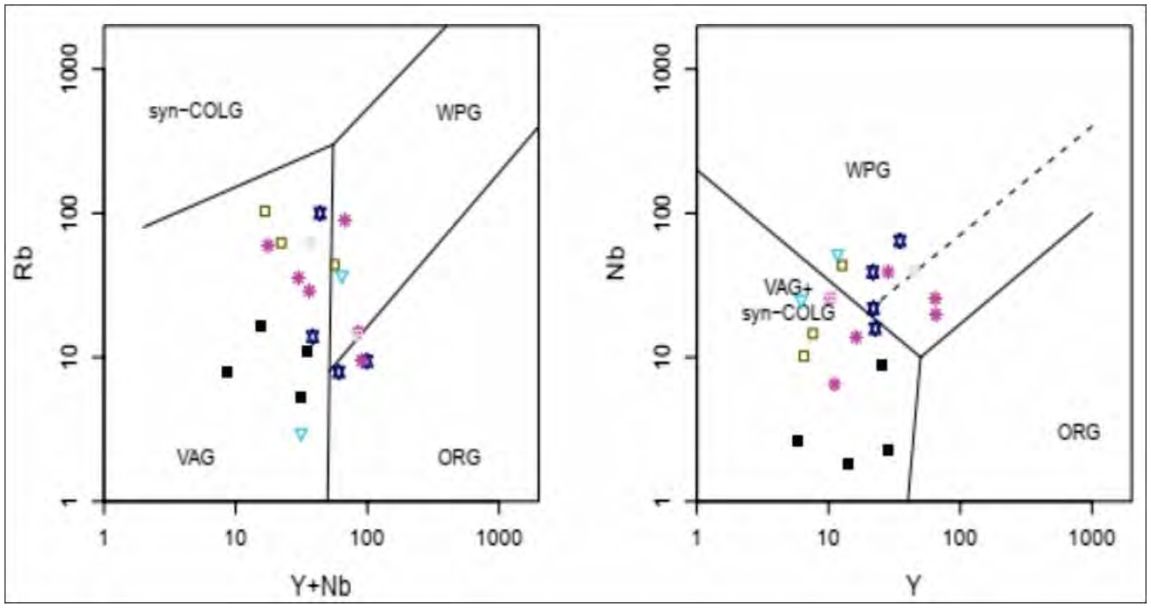

Figure 4.7. Tectonic discrimination diagrams for the study area (Pearce et al., 1984). Abbreviations- syn-COLG: Syn-collision Granites, ORG: Ocean Ridge Granites, VAG:

CONCLUSIONS

The findings of this study indicate that the rocks of the area have undergone fenitization and metasomatism processes. Fenitization is the process by which feldspar minerals in rocks are replaced by sodium-rich minerals, such as cancrinite, due to the influence of alkali-rich fluids. On the other hand, metasomatism is the alteration of rocks and minerals by the influx of fluids containing elements that can replace or modify the original minerals.

It is pertinent to mention that metasomatism occurs in intrusions of ijolite and carboantite. Ijolite is an intrusive igneous rock that is rich in sodium, titanium, and iron, while carboantite is a rare carbonate mineral that contains barium, strontium, and calcium. These rocks can replace or change the minerals present in the original rock as a result of the metasomatic fluids. As a consequence of these processes, minerals such as cancrinite and carbonate can form, which are typically found in the later stages of mineral replacement.

The alkaline magmatic fluids can alter both rocks and minerals. For example, cancrinite can replace primary nepheline, while randomly oriented carbonate veinlets can form due to the action of these fluids. Hydrothermal fluids produced by carbonatitic and silicate magma are responsible for metasomatism and rock alteration, indicating that their genesis should be linked to contact metasomatic processes. In this way, it is suggested that the alteration and replacement of rocks are a result of the action of these fluids.

It is concluded with a brief summary of the processes of fenitization and metasomatism in rocks and their significance in altering minerals and forming new ones. It highlights the role of alkaline magmatic fluids and hydrothermal fluids produced by carbonatitic and silicate magma in these processes, emphasizing their impact on rocks and minerals.

RECOMMENDATIONS

The present investigation has revealed that the rocks have undergone metasomatism and alteration, and a detailed examination of the mineral chemistry of selected minerals is recommended to further investigate the pressure-temperature conditions that existed during their formation. This will provide valuable information regarding the genesis and magmatic affiliation of the rocks.

Sphene and apatite are significant sources of rare earth elements (REEs) and can have high concentrations of these elements in alkaline rocks. The investigation of REE in alkaline rocks that contain sphene and apatite can provide important information about the potential for REE extraction and the geological processes that have led to their concentration.

Overall, the investigation of REE in alkaline rocks that contain sphene and apatite is important for understanding the geology and mineralogy of these rocks, as well as the potential for REE extraction.

In summary, this study has shed light on the geological processes that have shaped the study area and has provided important information that can inform future research and exploration efforts in this and other geological settings.

REFERENCES

Ahmad, M.I., 1951. Report on the Warsak hydroelectric project. Government of Pakistan.

Ahmad, M., Ali, K. S. S., Khan. B., M. A. and Ullah, I., 1969. The geology of the Warsak area, Peshawar, West Pakistan. Geol. Bull. Univ. Peshawar 4, 44-78.

Anczkiewicz, R., Oberli, F., Burg, J. P., Villa, I. M., Günther, D., & Meier, M. (2001). Timing of normal faulting along the Indus Suture in Pakistan Himalaya and a case of major 231Pa/235U initial disequilibrium in zircon. Earth and Planetary Science Letters, 191(1-2), 101-114.

Bard, J. P., Maluski, H., Matte, P. and Proust, F., 1980. The Kohistan sequence: crust and mantle of an obducted island arc. Geol. Bull. Univ. Peshawar, 11, 87-94.

Bard, J.P., 1983. Metamorphism of an obducted island arc: example of the Kohistan sequence (Pakistan) in the Himalayan collided range. Earth and Planetary Science Letters, 65(1): 133-144.

Beck, R.A., Burbank, D.W., Sercombe, W.J., Olson, T.L., Khan, A.M., 1995. Organic carbon exhumation and global warming during the early Himalayan collision. Geology, 23(5): 387-390.

Burchfiel, B. C., & Royden, L. H. (1985). North-south extension within the convergent Himalayan region. Geology, 13(10), 679-682.

Burrett, C.F., 1974. Plate tectonics and the fusion of Asia. Earth and Planetary Science Letters, 21(2): 181-189.

Borst, A. et al., 2016. Zirconosilicates in the kakortokites of the Ilímaussaq complex, South Greenland: Implications for fluid evolution and high-field-strength and rare-earth element mineralization in agpaitic systems. Mineralogical Magazine, 80(1): 5-30.

Butt, K., Arif, A.Z., Ahmed, J., Ahmed, A., Qadir, A., 1989. Chemistry and petrography of the Sillai Patti carbonatite complex, North Pakistan. Geol. Bull. Univ. Peshawar, 22: 197-215.

Chakhmouradian, A.R., Mitchell, R.H., 2002. The mineralogy of Ba-and Zr-rich alkaline pegmatites from Gordon Butte, Crazy Mountains (Montana, USA): comparisons between potassic and sodic agpaitic pegmatites. Contributions to Mineralogy and Petrology, 143(1): 93-114.

Chang, C.-f., Cheng, H.-l., 1973. Some tectonic features of the Mt. Jolmo Lungma area, southern Tibet, China. Scientia Sinica, 16(2): 257-265.

Chaudhry, M., Chaudhry, A., 1974. Geology of Khagram area, Dir district. Geol. Bull. Punjab Univ, 11: 21-43.

Chaudhry, M., Ashraf, M., Hussain, S., Iqbal, M., 1976. Geology and petrology of Malakand and a part of Dir (Toposheet 38 N/14). Geological Bulletin University of the Punjab, 12: 17-40.

Chaudhry, M. N., & Ghazanfar, M. (1990). Position of the Main Central Thrust in the tectonic framework of Western Himalaya. Tectonophysics, 174(3-4), 321-329.

Coulson, A. L., 1936. A soda-granite suit in the North-West Frontier Province. Proc. National Inst. Sci. India.2, 103-111.

Coward, M. et al., 1982. Geo-tectonic framework of the Himalaya of N Pakistan. Journal of the Geological Society, 139(3): 299-308.

Coward, M. P. 1984. The strain and textural history of thin-skinned tectonic zones: examples from the Assynt region of the Moine Thrust zone NW Scotland. J. Struct. Geol. 6, 89-99.

Coward, M. P., & Butler, R. W. H. (1985). Thrust tectonics and the deep structure of the Pakistan Himalaya. Geology, 13(6), 417-420.

Coward, M., Butler, R., Khan, M.A., Knipe, R., 1987. The tectonic history of Kohistan and its implications for Himalayan structure. Journal of the Geological Society, 144(3): 377-391.

Coward, M. P., Butler, R. W. H., Chambers, A. F., Graham, R. H., Izatt, C. N., Khan, M. A., ... & Williams, M. P. (1988). Folding and imbrication of the Indian crust during Himalayan collision. Philosophical Transactions of the Royal Society of London. Series A, Mathematical and Physical Sciences, 326(1589), 89-116.

DiPietro, J. A., & Pogue, K. R. (1999). Geologic map of the Indus syntaxis and surrounding area. Himalaya and Tibet: mountain roots to mountain tops, 328, 159.

DiPietro, J. A., Hussain, A., Ahmad, I., & Khan, M. A. (2000). The Main Mantle Thrust in Pakistan: its character and extent. Geological Society, London, Special Publications, 170(1), 375-393.

Srivastava, R. K., Heaman, L. M., Sinha, A. K., & Shihua, S. (2005). Emplacement age and isotope geochemistry of Sung Valley alkaline–carbonatite complex, Shillong Plateau, northeastern India: implications for primary carbonate melt and genesis of the associated silicate rocks. Lithos, 81(1-4), 33-54.

Elliott, H., Gernon, T., Roberts, S., Hewson, C., 2015. Basaltic maar-diatreme volcanism in the Lower Carboniferous of the Limerick Basin (SW Ireland). Bulletin of Volcanology, 77(5): 1-22.

Elliott, H. et al., 2018. Fenites associated with carbonatite complexes: A review. Ore Geology Reviews, 93: 38-59.

Frost, B. R., & Frost, C. D. (2008). A geochemical classification for feldspathic igneous rocks. Journal of Petrology, 49(11), 1955-1969.

Gansser, A., 1964. Geology of the Himalayas. pp. 298 (Wiley Interscience) London.

Gansser, A., 1980. The significance of the Himalayan suture zone. Tectonophysics, 62(1-2): 37-52.

Graser, G., Markl, G., 2008. Ca-rich ilvaite–epidote–hydrogarnet endoskarns: A record of late-magmatic fluid influx into the persodic Ilímaussaq Complex, South Greenland. Journal of Petrology, 49(2): 239-265.

Heim, A., and Gansser, A., 1939. Central Himalaya: Geological observations of Swiss expedition 1936; Reprinted Delhi Hind. Publ. Co. 246.

Hodges, K.V., 2000. Tectonics of the Himalaya and southern Tibet from two perspectives. Geological Society of America Bulletin, 112(3): 324-350.

Holub, F.V. et al., 2010. Petrology and geochemistry of the Tertiary alkaline intrusive rocks at Doupov, Doupovské hory Volcanic Complex (NW Bohemian Massif). Journal of Geosciences, 55(3): 251-278.

Howie, R., Zussman, J., Deer, W., 1992. An introduction to the rock-forming minerals. Longman London, UK.

Hsü, K.J., Guitang, P., Sengör, A., 1995. Tectonic evolution of the Tibetan Plateau: A working hypothesis based on the archipelago model of orogenesis. International Geology Review, 37(6): 473-508.

Jan, M.Q., 1980. Petrology of the obducted mafic ultramafic metamorphites from the southern part of the Kohistan Isalnd arc sequence. International committee on Geodynamics Group 6 Meeting 1977 Peshawar, p. 95-107; Peshawar.

Jan, M.Q., 1981a. Tectonic subdivision of granitic rocks of Northern Pakistan. Geol. Bull. Univ. Peshawar, 14: 159-182.

Jan, M.Q., Karim, A., 1990. Continental magmatism related to late paleozoic-early mesozoic rifting in northern Pakistan and kashmir. Journal Of Himalayan Earth Sciences, 23.

Kempe, D., Jan, M.Q., 1970. An alkaline igneous province in the North-West Frontier province, West Pakistan. Geological Magazine, 107(4): 395-398.

Kempe, D.R.C., MQ, J., 1980. The Peshawar plain alkaline igneous province, NW Pakistan.

KEMPE, D.C., 1983. Alkaline granites, syenites, and associated rocks of the Peshawar Plain alkaline igneous province, Northwest Pakistan, Granites of Himalaya Karakorum and Hindu Kush, pp. 143-169.

Khan, A., Aslam, M., Khan, R. N., 1995. Regional Geological Map of the Jamrud Quadrangle, Khyber Agency, NWFP, Pakistan. GSP map (scale 1:50,000).

Khan, M.A. et al., 1998. Geology of the Chalt–Babusar transect, Kohistan terrane, N. Pakistan: implications for the constitution and thickening of island-arc crust. Journal of Asian Earth Sciences, 16(2-3): 253-268.

Khattak, N. U., Qureshi, A. A., Akram, M., Khan, M. A., Qureshi, I. E., Mehmood, K., & Khan, H. A. (2001). Unroofing history of the Sillai Patti granite gneiss, Pakistan: constraints from zircon fission-track dating. Radiation measurements, 34(1-6), 409-413.

Khattak, N. et al., 2005. Unroofing history of the Jambil and Jawar carbonatite complexes from NW Pakistan: constraints from fission-track dating of apatite. Journal of Asian Earth Sciences, 25(4): 643-652.

Khattak, N. U., Akram, M., Khan, M. A., & Khan, H. A. (2008). Emplacement time of the Loe–Shilman carbonatite from NW Pakistan: Constraints from fission-track dating. Radiation measurements, 43, S313-S318.

Kogarko, L., Lahaye, Y., Brey, G., 2010. Plume-related mantle source of super-large rare metal deposits from the Lovozero and Khibina massifs on the Kola Peninsula, Eastern part of Baltic Shield: Sr, Nd and Hf isotope systematics. Mineralogy and Petrology, 98(1): 197-208.

Le Bas, M., 1987. Nephelinites and carbonatites. Geological Society, London, Special Publications, 30(1): 53-83.

Le Bas, M., Mian, I., Rex, D., 1987. Age and nature of carbonatite emplacement in North Pakistan. Geologische Rundschau, 76(2): 317-323.

Le Bas, M.J., 2008. Fenites associated with carbonatites. The Canadian Mineralogist, 46(4): 915-932.

Le Fort, P. (1975). Himalayas: The collided range, present knowledge of the continental arc. American Journal of Science, 275(1), 1-44.

Le Fort, P. (1986). Metamorphism and magmatism during the Himalayan collision. Geological Society, London, Special Publications, 19(1), 159-172.

Martin, R. F., Siddique, S. F. A. and King, B. H., 1962. A geological reconaissance of the region between the Lower Swat and Indus River of Pakistan. Geol. Bull. Punjab. Univ. 2, 1-14.

Mariano, A., 1983. Fenitization in alkaline rocks, 1983 MSA Symposium, Wisconsin.

MARKS, M., VENNEMANN, T., SIEBEL, W., MARKL, G., 2003. Quantification of magmatic and hydrothermal processes in a peralkaline syenite–alkali granite complex based on textures, phase equilibria, and stable and radiogenic isotopes. Journal of Petrology, 44(7): 1247-1280.

McDonough, W. F., Sun, S. S., Ringwood, A. E., Jagoutz, E., & Hofmann, A. W. (1992). Potassium, rubidium, and cesium in the Earth and Moon and the evolution of the mantle of the Earth. Geochimica et Cosmochimica Acta, 56(3), 1001-1012.

Morogan, V., 1994. Ijolite versus carbonatite as sources of fenitization. Terra Nova, 6(2): 166-176.

Petterson, M.G., Windley, B.F., 1985. RbSr dating of the Kohistan arc-batholith in the Trans-Himalaya of north Pakistan, and tectonic implications. Earth and Planetary Science Letters, 74(1): 45-57.

Qureshi, A. A., Beg, M. I., & Babar, A. N. (1980, October). The radioactive carbonatite of Loe-Shiiman. In PAEC-KFK Seminar.

Rafiq, M., Ali, A., Ali, S., 2005. Petrography of alkaline-igneous complex from Michini, Mohmand Agency, NWFP, Pakistan. Geol Bull Univ Peshawar, 38: 81-88.

Rass, I., Abramov, S., Utenkov, V., Kozlovskii, V., Korpechkov, D., 2006. Role of fluid in the genesis of carbonatites and alkaline rocks: geochemical evidence. Geochemistry International, 44(7): 636-655.

Schilling, J., Marks, M.A., Wenzel, T., Markl, G., 2009. Reconstruction of magmatic to subsolidus processes in an agpaitic system using eudialyte textures and composition: a case study from Tamazeght, Morocco. The Canadian Mineralogist, 47(2): 351-365.

Searle, M., Khan, M.A., Fraser, J., Gough, S., Jan, M.Q., 1999. The tectonic evolution of the Kohistan- Karakoram collision belt along the Karakoram Highway transect, north Pakistan. Tectonics, 18(6): 929-949.

Searle, M. P., & Treloar, P. J. (2010). Was Late Cretaceous–Paleocene obduction of ophiolite complexes the primary cause of crustal thickening and regional metamorphism in the

Pakistan Himalaya?. Geological Society, London, Special Publications, 338(1), 345-359.

Sengör, A.C., 1984. The Cimmeride orogenic system and the tectonics of Eurasia. Geol. Soc. Amer. Spec. Pap. 195, 82 pp.; Tulsa.

Sengör, A., Altiner, D., Cin, A., Ustaomer, T., Hsu, K., 1988. Origin and assembly of the Tethyside orogenic collage at the expense of Gondwana Land.

Sengör, A.C., Natal'in, B.A., 1996. Turkic-type orogeny and its role in the making of the continental crust. Annual Review of Earth and Planetary Sciences, 24(1): 263-337.

Shand, S. J., 1943, Eruptive rocks: Their genesis, composition, classification, and their relation to ore-deposits with a chapter on meteorite, John Wiley & Sons.

Siddiqui, S., 1965. Alkaline Rocks of Chamla, Swat. Geol. Bull. Panjab Univ., 5: 52.

Siddiqui, S., 1967. Note on the discovery of carbonatite rocks in the Chamla area, Swat State, West Pakistan. Geol. Bull. Panjab Univ., 6: 85.

Sørensen, H., 1974. The Alkaline Rocks. 622 pp. John Wiley & Sons, London.

Srivastava, R.K., Heaman, L.M., Sinha, A.K., Shihua, S., 2005. Emplacement age and isotope geochemistry of Sung Valley alkaline–carbonatite complex, Shillong Plateau, northeastern India: implications for primary carbonate melt and genesis of the associated silicate rocks. Lithos, 81(1-4): 33-54.

Tahirkheli, R.A.K., Mattauer, M., Proust, F., and Tapponnier, P., 1979, The India-Eurasia suture zone in northern Pakistan; synthesis and interpretation of recent data at plate scale, *in* Farah, A., and De Jong, K.A., eds., Geodynamics of Pakistan: Quetta, Geological Survey of Pakistan, p. 125–130.

Tahirkheli, R.A.K., 1982. Geology of the Himalaya, Karakoram and Hindukush in Pakistan. Geol. Bull. Peshawar Univ. 15: 51 pp.; Peshawar.

Tahirkheli, T., Asif Khan, M., Ihsanullah, M., 1990. A-type granites of Warsak, Khyber Agency, N. Pakistan: Rift-related acid magmatism in the Indian Plate. Geological Bulletin of the University of Peshawar, 23: 187-202.

Thakur, V. C. (1981). Regional framework and geodynamic evolution of the Indus-Tsangpo suture zone in the Ladakh Himalayas. Earth and Environmental Science Transactions of The Royal Society of Edinburgh, 72(2), 89-97.

Treloar, P.J. et al., 1989. K- Ar and Ar- Ar geochronology of the Himalayan collision in NW Pakistan: Constraints on the timing of suturing, deformation, metamorphism and uplift. Tectonics, 8(4): 881-909.

Valdiya, K. S., Malinconico, L. L., & Lillie, R. J. (1989). Trans-Himadri intracrustal fault and basement upwarps. Tectonics of the Western Himalaya, 232, 153-168

Verwoerd, W. J. (1967). The carbonatites of South Africa and South West Africa. Handbk. Geol. Surv. S. Afr., 6, 452 pp.

Wooleÿ, A., Kempe, D., 1989. Carbonatites: nomenclature, average chemical compositions and element distributions. Carbonatites—genesis and evolution/Ed. K. Bell. Unwin Hyman: 1-14.

Yin, A., Harrison, T.M., 2000. Geologic Evolution of the Himalayan-Tibetan Orogen. Annual Review of Earth and Planetary Sciences, 28(1): 211-280.

ZharikovF, V., 2007. 9. Metasomatism and metasomatic rocksF. A classification of metamorphic rocks and glossary of terms. Recommendations of the International Union of Geological Sciences Subcommission on the Systaematics of Metamorphic Rocks.